Cross section measurements of deuteron induced reactions

Laboratory of Cyclotron and Fast Neutron Generators

Eva Šimeková

Proposal ID

58

The proton and deuteron induced activation reactions have a great interest for the assessment of induced radioactivity in the accelerator components, targets and beam stoppers as well as isotope production for medicine. The description of deuteron-nucleus interaction represents important tests for both the quality of reaction mechanism models and evaluation of nuclear data request especially for fusion reactor technology.

3.4.2013

Two runs were realized. In the first one a Cr foil (together with Al foils serving for beam energy attenuation and as an additional monitor) was irradiated by deuteron with initial energy 19.62 MeV during 446 s with a mean current 0.16 μA. The stacked–foil activation technique was utilized to irradiate Zn foils (initial deuteron beam energy 19.62 MeV, irradiation time 634 s, mean current 0,16 μA) in the second run. The foil activities were measured by two HPGe detectors and are processed now. The excitation functions for production of 65,66,67,68Ga, 71m,72Zn and 61,64Cu should be obtained.

20.11.2013

In previous experiments we obtained excitation function of proton induced reactions on natural iron for 56Co, 56Mn, 54Mn, 52mMn, 52Mn, 55Co, 58mCo, 58gCo and 53m+gFe isotopes in proton energy range up to 20 MeV, the cross section for the natFe(p*)56Mn, natFe(p*)52mMn, natFe(p*)58mMn and natFe(p*)58gMn reactions were obtained for the first time. In this experiment we continued the measurements with proton energy up to 30.525 MeV. The main reason for an extension of proton energy region is a discrepancy in cross sections for the natFe(p,*)54Mn reaction between different authors in proton energy region of about 20 MeV. The induced activities measurements by two HPGe detectors proceed now.

Mesostructure and fractal properties of the carbonic molecular sieves

Neutron Physics Laboratory - Neutron diffraction

Evgeny Velichko

Proposal ID

57

EXPERIMENTAL REPORT

Title. Mesostructure and fractal properties of the carbonic molecular sieves

Objectives. The experiment aims the structural characterization of new material made on the base of anthracite. Samples were prepared by annealing with different conditions and possess different characteristics of the gas sorption activity. The experiment goal was to uniquely determine by non-destructive method (USANS) the relationship between the mesostucture of the sample and it's sorption activity.

Experiment

1. Samples. There were 5 samples prepared with different conditions: sample 1 was the initial anthracite material grinded in the mortar into powder with particle sizes 1mkm; sample 2 was the initial anthracite material grinded into powder with particle sizes 31.5-100mkm; sample 3 was the low-temperature activated anthracite powder with particle sizes 31.5-100mkm in the air environment; sample 4 was the high-temperature activated anthracite powder with particle sizes 31.5-100mkm with 2h activation time; sample 5 was the high-temperature activated anthracite powder with particle sizes 31.5-100mkm with 5h activation time.

2. Ultra small-angle neutron scattering. The USANS experiment was performed at the double-crystal diffractometer MAUD of LVR-15 research reactor in Prague (Czech Republic), which using neutrons with the wavelengths $\lambda = 2.09$ nm ($\Delta\lambda/\lambda = 0.18$). The range of momentum transfer $2 \times 10^{-4} < Q < 2 \times 10^{-2}$ Å^{-1}. All measurements were made at room temperature.

Achievements and Main Results.

The inner structure of the carbonic molecular sieves was studied by USANS method. There are scattering curves in double logarithmic scale on the figure 1. These data clearly demonstrates that all samples are of fractal nature with different fractal dimensions. Parameters of the samples are summarized in the Table 1.

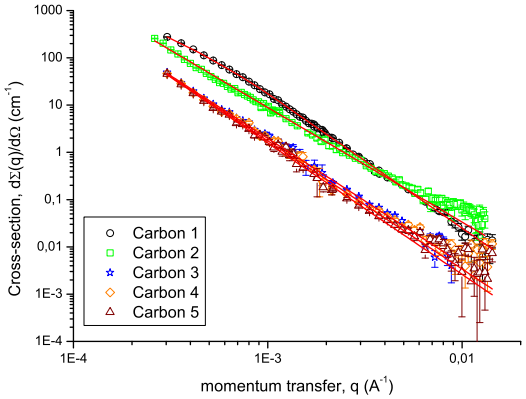

Figure 1: The USANS cross section dΣ(q)/dΩ for the samples of carbonic molecular sieves

.

Table 1: Parameters of the CMS samples

Sample number	1	2	3	4	5
D_S=6-Δ	2.15±0.05	2.58±0.05	2.28±0.05	2.35±0.05	2.22±0.05
A1, cm^{-2}g^{-1}	756±44	-	-	-	-
A2(D$_S$),×10^8,cm^{2}g^{-1}	5.0±0.3	47.5±5	1.26±0.2	2.18±0.2	0.71±0.01
R$_g$,Å	6000±200	-	-	-	-

The treatment of USANS data for samples of artificial opal and interpretation of all the obtained data is still in progress.

Study of alpha particle induced reactions on 226Ra

Laboratory of Cyclotron and Fast Neutron Generators

Ján Kozempel

Proposal ID

53

ČESKÉ
VYSOKÉ UČENÍ
TECHNICKÉ V PRAZE

Fakulta jaderná
a fyzikálně
inženýrská

Katedra jaderné chemie, Břehová 7 115 19 Praha 1

Č. j. 003-01/13/14115/K

We hereby request the cancelation of allocated beam-time for our experiment of ^{226}Ra irradiation.

In our first experiments we have found that the production of ^{227}Th via the ^{226}Ra(α,3n)^{227}Th is feasible. However precise measurement of cross-sections for ^{227}Th production at given experimental limits (I ≤ 1 μA, mass of ^{226}Ra ≈ 44 μg) is practically impossible using both gamma and alpha spectroscopies (due to high background levels). To solve this problem we propose 1) increase beam currents, 2) subsequent separation of ^{227}Th from ^{226}Ra target material, 3) detection of ^{227}Th via direct method (ICP-MS).

In order to elaborate such new methods for precise ^{227}Th yield estimation we request the cancelation of currently allocated beam-time and postpone it, until we confirm that we would be able to use newly developed methods.

Effect of high LET radiation on specific interaction of proteins with DNA.

Laboratory of Cyclotron and Fast Neutron Generators

Marie Davidkova

Proposal ID

52

The project “Effect of high LET radiation on specific interaction of proteins with DNA” is a contribution of our laboratory to the international COST project MP1002 "Nano-scale insights in ion beam cancer therapy (Nano-IBCT)“. The laboratory is a member of working group WG5 Radiobiological effects (detection of DNA double strand breaks, prediction and cell damage). The goal of the project is to determine how radiation damage of repair proteins influences rate and fidelity of repair mechanisms in cells. Irradiation of biological samples at accelerators of the Nuclear Physics Institute ASCR in Řež (cyclotron U120M and tandetron) is specific by low energies of incident proton beam. Maximal proton energy at cyclotron U120M is approximately 34 MeV, at tandetron 6 MeV. The range of these ions in water is only several tens of micrometers (range of 6 MeV protons in water is approximately 0.5 mm, in case of 34 MeV protons about 11 mm). Therefore, the experiments should be performed with thin biological samples.

Several particular experimental setups has been designed and tested:
a) own developed prototype rings from plastic or metal extending thin Mylar foil
b) sterile Petriho dishes with glass bottom
c) commercially available plastic dishes with cover and bottom from Mylar foil (Chemplex, USA).
As the best solution for further experiments with neonatal dermal fibroblasts seems the last proposed setup using plastic dishes. Petri dishes with glass bottom will be used for experiments with our colleagues from Biophysical Institute ASCR, which analyze irradiated samples by FISH technique (fluorescence in situ hybridization). Cells are seeded 24 h before irradiation and grown directly on glass slide. DNA plasmids in water solution are irradiated in thin plastic tubes.

The proportion of direct and indirect effects in proton tracks has been followed in pBR322 DNA plasmids in water solution. Samples were irradiated in presence of increasing concentrations of OH radical scavengers (coumarin-3-carboxylic acid, dimethylsulfoxid or glycylglycine). The yields of single and double DNA strand breaks were determined by agarose gel electrophoresis. The contributions of direct and indirect DNA damage in dependence on scavenger concentration has been determined for 30 MeV protons. The experiments will be extended for larger interval of proton energies and also other types of ions.

Radiation damage to proteins has been studied for selected restriction enzymes HindIII and PvuII. Enzymes irradiated by increasing doses were subsequently with DNA pCDNA3 plasmids. Restriction enzymes recognize and cleave specific DNA base sequences. The functionality of irradiated restriction enzymes can be thus followed by agarose gel electrophoresis, where DNA fragments of known size can be easily visualized. Decrease of enzyme activity with increasing absorbed dose has been detected.

During the first year of the project, the results for cell cultures have not been planned. In the frame of planning of experimental studies, methods and experimental setup has been proposed and prepared. The first pilot experiments have been realized too. Cell survival curves have been determined for confluent neonatal fibroblasts grown on 2.5 μm Mylar foils and irradiated by gamma radiation and 15 and 30 MeV protons. In irradiated samples the cell survival and micronuclei formation has been determined. Experiments will be repeated, extended and analyzed. In collaboration with Biophysics Institute ASCR, the first experiments focused to DSB repair in normal neonatal skin fibroblasts have been performed.

An investigation of the low temperature magnetic structures of Mn3Ni20P6 using neutron diffraction

Neutron Physics Laboratory - Neutron diffraction

Viktor Höglin

Proposal ID

51

Report regarding proposal "An investigation of the low temperature magnetic structures of $Mn_3Ni_{20}P_6$ using powder neutron diffraction"

V. Höglin, M. Sahlberg, P. Nordblad, Y. Andersson, Uppsala University, Sweden
P. Beran, Nucl. Physics Inst., Rez, Czech Republic

Examples of the complex behavior of manganese compounds are the two isostructural compounds $Mn_3Pd_{20}P_6$ and $Mn_3Ni_{20}P_6$, which both crystallize in the ordered $Cr_{23}C_6$-type structure, with the unit cell parameter 11.9563(2) Å and 11.0820(2) Å, respectively [1]. $Mn_3Pd_{20}P_6$ orders ferromagnetically below 110K and shows an unusual temperature dependence of the saturation moment at lower temperatures. $Mn_3Ni_{20}P_6$ shows a very weak ferrimagnetic order at low temperatures and shows an unexplained anomaly in the macroscopic magnetic response around 30K, see Fig 1. Between 26K and 30K a commensurate anti-ferromagnetic ordering occurred with the propagation vector (0, 0 ,½).

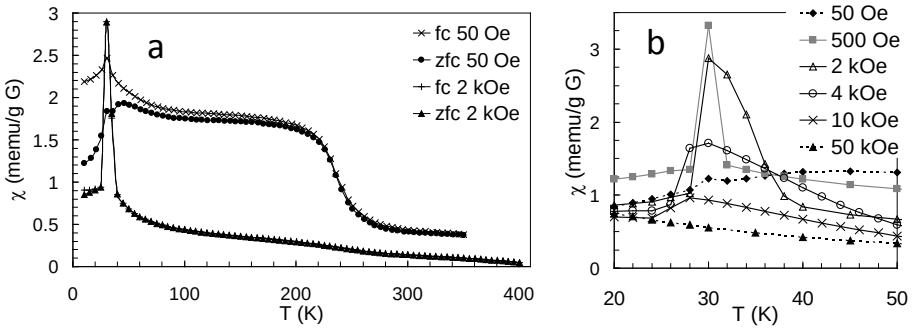

Fig 1. a)Temperature dependence of field-cooled (fc) and zero-field-cooled (zfc) magnetic susceptibility (w ¼ M=H) in applied field of 50 Oe and 2 kOe, respectively. b) Close-up of the low-field anomaly around 30K, in applied fields 50 Oe–50 kOe.

Neutron powder diffraction experiments were performed on $Mn_3Ni_{20}P_6$ at 298 K, 30 K, 26 K, 20 K and 4 K using the MEREDIT instrument. The motivation for the experiments was to investigate the complex antiferromagnetic magnetic structures of $Mn_3Ni_{20}P_6$ below 30 K.

The extracted data is still under evaluation but preliminary results propose an incommensurate magnetic ordering below 26K with the propagation vector (0,0,0.463) and the magnetic moments 4.2(2) μ_B and 4.8(1) μ_B on the two manganese positions. Observed and calculated neutron powder diffraction profiles are shown in fig. 2. The preliminary proposed magnetic structure is shown in fig 3.

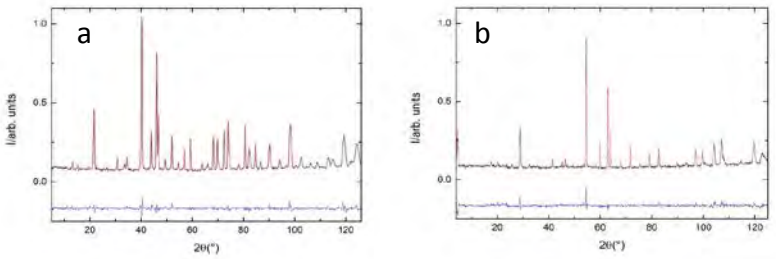

Fig 2 a)Neutron powder diffraction profile at 298K = 1.46 Å. b) Neutron powder diffraction profile at 4K with λ = 1.95 Å.

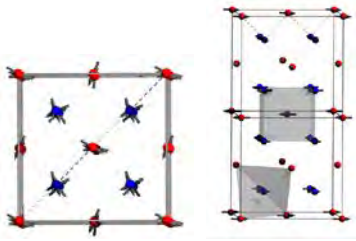

Fig. 3. The proposed incommensurate magnetic structure of $Mn_3Ni_{20}P_6$ at 4K projected along the c-axis and the a-axis, respectively.

Reference

1.T. Eriksson, M. Vennström, S. Ronneteg, Y. Andersson, P. Nordblad, J. Magn. Magn. Mater. 308 (2007) 203.

Determination of an initial Ni:Ti ratio influence on phase composition of products during reactive s

Neutron Physics Laboratory - Neutron diffraction

Alena Michalcová

Proposal ID

49

Final Report: Determination of an initial Ni:Ti ratio influence on phase composition of products during reactive sintering of NiTi intermetallic alloy

The aim of this project was to obtain information about phase composition of NiTi alloys by means of neutron powder diffraction and it was absolutely accomplished. The alloys with nominal powder compositions Ni:Ti of 50:50, 51:49, 52:48, 53:47, 54:46 and 55:45 were prepared be reactive sintering. These samples had inhomogeneous structure with coarse matrix grains, which together with bad scattering properties of NiTi phase disabled them to be studied by X-ray diffraction. This problem was successfully solved by utilization of neutron powder diffraction. The obtained results showed that the content of unwanted Ti2Ni intermetallic phase remained constant without t the influence of initial Ni: Ti ratio. It was also proven that with increasing Ni content another intermetallic phase (Ni4Ti3) occurred and the NiTi matrix contained areas rich in Ni. These results are in excellent agreement with microscopy results and give them satisfying explanation (e.g. the reason for different matrix colour in some places, which is caused by Ni enrichment).

Based on the results from neutron powder diffraction, it is obvious that some new technology like thermal or thermo-mechanical treatment of equimolar Ni-Ti alloy has to be suggested for obtaining homogenous material formed exclusively by NiTi solid solution. This project has confirmed the great feasibility of neutron powder diffraction for investigation of NiTi alloys.

Having the experience reached by this project, our team is planning to apply Canam proposal for neutron powder diffraction in case of thermally and thermo-mechanically treated samples.

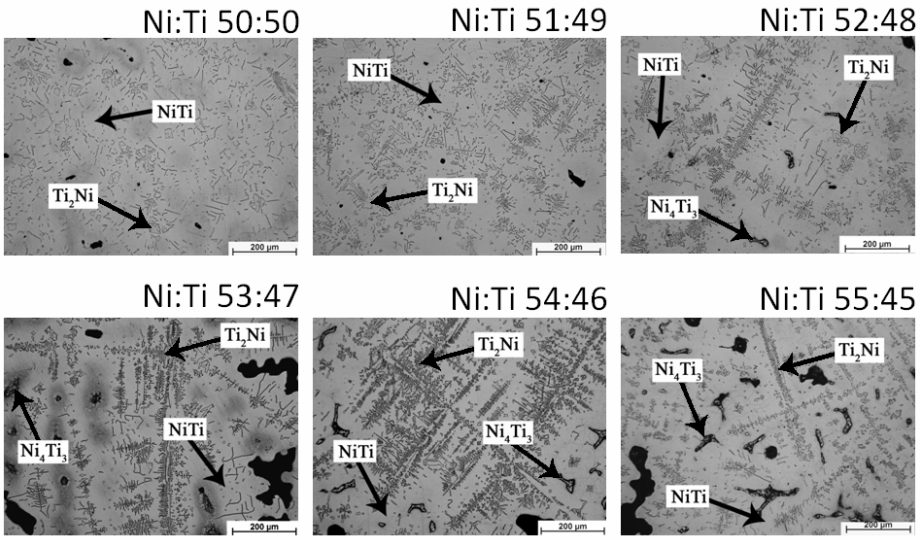

Fig. 1. Light micrographs of NiTi alloys.

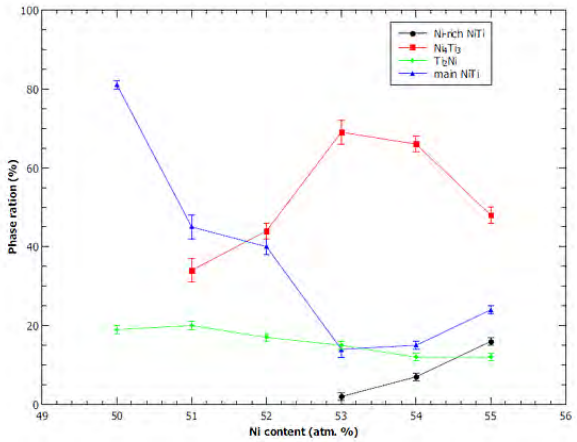

Fig. 2. Evolution of phase ration as a function of composition determined by neutron powder diffraction.

Cross section measurements of deuteron induced reactions

Laboratory of Cyclotron and Fast Neutron Generators

Eva Šimeková

Proposal ID

48

The proton and deuteron induced reactions are of a great interest for the assessment of induced radioactivity of accelerator components, targets and beam stoppers. Continuing our previous deuteron activation measurements on Al, Cu, Fe and Co, we measured excitation functions of reactions on Mn, Cr, W and Zr provoked by deuterons up to 20 MeV in three irradiations.

6.2.2013
We realized two runs. In the first one a Cr foil (together with Al foils serving for beam energy attenuation and as an additional monitor) was irradiated by deuteron with initial energy 19.76 MeV during 5 min with a mean current 0.15 μA. The stacked–foil activation technique was utilized to irradiate Mn foils (initial deuteron beam energy 19.76 MeV, irradiation time 5 min, mean current 0.32 μA) in the second run. The excitation function for 55Mn(d,p)56Mn 55Mn(d,2np+)54Mn and 55Mn(d,4np+)52Mn were provided for the deuteron energy range 2-20 MeV.

28.8.2013
Two runs were realized. It was performed a run (initial deuteron energy 20.09 MeV, similar condition as 6.2.2013) to irradiate single Cr foil and a stacked-foil activation technique was utilized to irradiate W foils in the second run. The foil activities measured by two HPGe detectors are processed now.

9.10.2013
Two runs were realized. It was performed a run (initial deuteron energy 20.025 MeV, similar condition as 6.2.2013) to irradiate single Cr foil and a stacked-foil activation technique was utilized to irradiate Zr foils in the second run. The activity measurements are proceeded to obtain values for long living isotopes.

We obtained cross section values for for 48V, 49Cr 52mMn, 52Mn, 54Mn generated by deuteron induced reactions on Cr.

Fractal organization of native chromatin in cell nuclei

Neutron Physics Laboratory - Neutron diffraction

Evgeny Velichko

Proposal ID

73

EXPERIMENTAL REPORT

Title. Fractal organization of native chromatin in cell nuclei

Objectives. The experiment aims the structural characterization of the chromatin arrangement in the intact biological cell nuclei, focusing on the question of nucleocome state and small-scale arrangement and their relation with the large-scale chromatin structure. We used osmotic shrinkage of the nucleus to directly change the volume constrains on chromatin chromatin packing and investigate their effect on structure.

Experiment

1. Samples. Cell nuclei were isolated, fixed by gluthar aldehyde and suspended (5-20 % by weight) in D_2O buffer. Half of the samples were osmotically dehydrated prior to fixation.

2. Ultra small-angle neutron scattering. The USANS experiment was performed at the double-crystal diffractometer MAUD of LVR-15 research reactor in Prague (Czech Republic), which using neutrons with the wavelengths $\lambda = 2.09$ nm. The range of momentum transfer $2 \times 10^{-4} < Q < 2 \times 10^{-2}$ Å^{-1}. All measurements were made at room temperature.

Achievements and Main Results.

The inner structure of the intact cell nuclei was studied by USANS method. There are scattering curves in double logarithmic scale on the figure 1. These data clearly demonstrates that all samples have complex structure. For all samples in the Q-range from 4×10^{-3} Å^{-1} to 2×10^{-2}Å^{-1}, the relationship between differential cross section and the scattering vector follows the power law $d\Sigma(q)/d\Omega$ Q^{-D} and thus can be linearised when plotted in double-logarithmic scale with the slope of the linear fit D 1.9. For samples 1 and 4 this power low dependence remains in the lowest Q-region, but for samples 2 and 3 in the Q-range less than 4×10^{-3}Å^{-1} the dependence of differential cross section of Q follows the Guinier law. From this dependency we obtain the gyration radii $R_g = 0.75\mu$m and 1.05μm for samples 2 and 3 respectively. For the $Q > 2 \times 10^{-2}$Å^{-1} the differential cross section for all the samples decays dramatically with increasing of Q. This complex behaviour of the differential cross section requires deep analysis and remains unexplained yet.

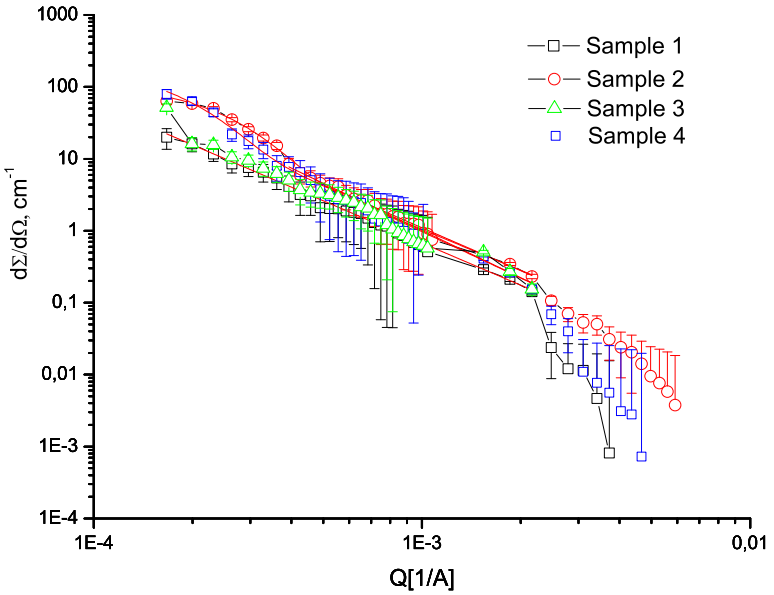

Figure 1: The USANS cross section $d\Sigma(q)/d\Omega$ for the samples of chicken erythrocyte cell nuclei

.

Neutron diffraction in welded and fatigued steels

Neutron Physics Laboratory - Neutron diffraction

Evangelos Hristoforou

Proposal ID

71

The present report refers to the determination of the residual stress values along the surface of welded ferromagnetic steels, by using three different techniques: X-ray diffraction, neutron diffraction and magnetic Barkhausen noise. The latter in not an established method for measuring the lattice stains and determining the corresponding stress values.

Three different grades of ferromagnetic steel were tested: (1) non-oriented electrical steel (2) low carbon (mild) steel: AISI 1008 and (3) low alloyed carbon steel: AISI 4130. For each grade of steel, two identical sheets were welded together in a butt joint configuration. The direction of the welding, in NOES samples, was perpendicular to the rolling direction, whereas, in both AISI 1008 and AISI 4130 samples this was parallel to the rolling direction.

Stress measurements on the surface of the test samples were conducted with the Magnetic Barkhausen Noise (MBN) technique, as well as, the X-ray (XRD) and the neutron[1] diffraction methods. The determination of the residual stresses with the neutron diffraction method is not straightforward. The crystal lattice deformations were determined through the relevant measurements on the surface of a polycrystalline material, due to the presence of stress. Then, the residual stresses were calculated by using a suitable mathematical relationship. An example of the ND monitored residual stress distribution on the surface of the welded AISI 1008 sample is shown in Fig. 1. Figure 2 illustrates cross-plotting of the residual stress measurements by MBN, neutron and XRD diffraction on EBW welded AISI 4130 sample and TIG welded AISI 4130 sample

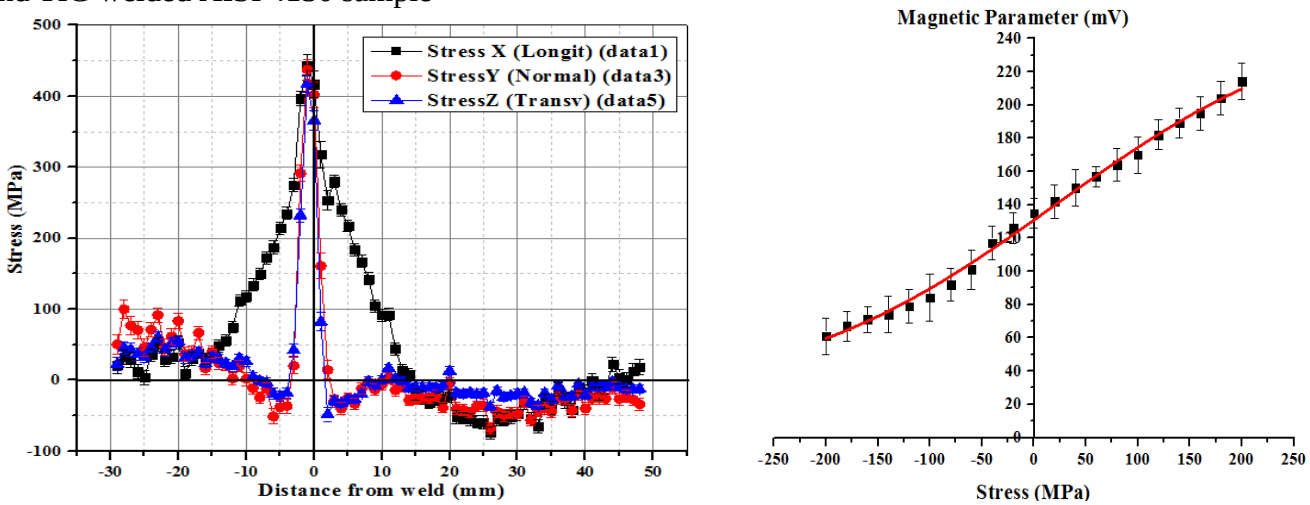

Figure 1: *Distribution of the residual stress values determined by the neutron diffraction measurements, on the surface of the AISI 1008 welded sample (left). Calibration of the stresses against magnetic permeability (right)*

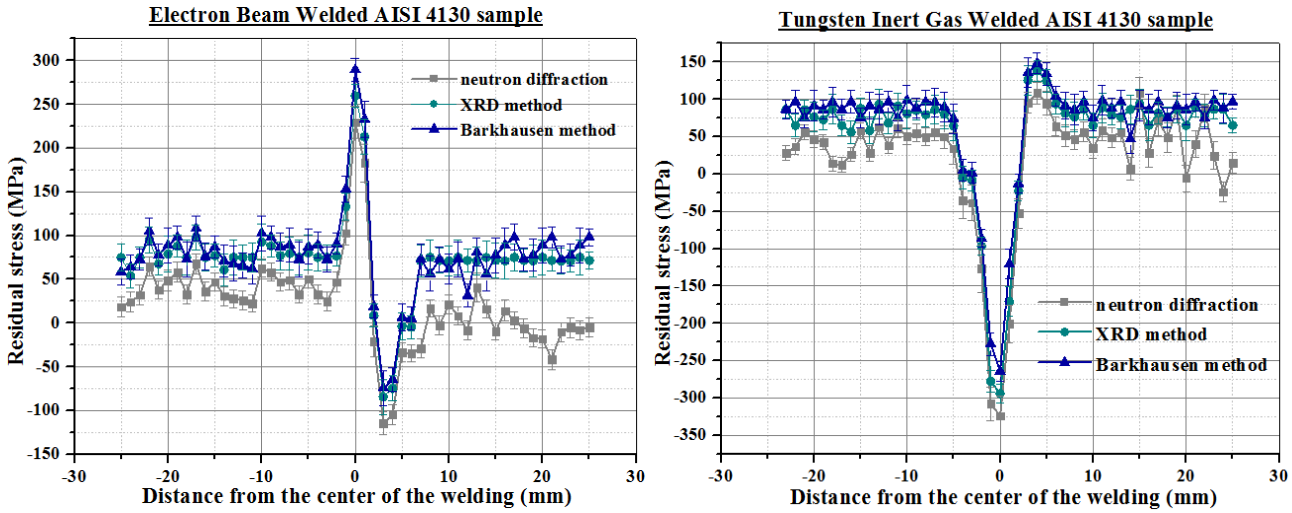

Figure 2: *Cross-plotting of the residual stress measurements by magnetic Barkhausen noise, neutron and XRD diffraction on the EBW welded AISI 4130 sample and (c) TIG welded AISI 4130 sample.*

[1] The low thickness and the dimensions of the welded NOES samples did not allow the measurement of the residual stress with the neutron diffraction method: the determination of the residual stress was conducted with MBN and XRD methods. In the present report, only the experimental results from the welded AISI 1008 and AISI 4130 samples are valid.

Conductivity of boron-doped polycrystalline diamond films: influence of specific boron defects

Neutron Physics Laboratory - Nuclear analytical methods with neutrons

Petr Ashcheulov

Proposal ID

70

Eur. Phys. J. B (2013)
DOI: 10.1140/epjb/e2013-40528-x

THE EUROPEAN PHYSICAL JOURNAL B

Regular Article

Conductivity of boron-doped polycrystalline diamond films: influence of specific boron defects

P. Ashcheulov[1,2], J. Šebera[1], A. Kovalenko[1], V. Petrák[1,3], F. Fendrych[1], M. Nesládek[4], A. Taylor[1], Z. Vlčková Živcová[5], O. Frank[5], L. Kavan[5], M. Dračínský[6], P. Hubík[7], J. Vacík[8], I. Kraus[2], and I. Kratochvílová[1,a]

[1] Institute of Physics, Academy of Sciences Czech Republic v.v.i, Na Slovance 2, 182 21 Prague 8, Czech Republic
[2] Faculty of Nuclear Physics and Physical Engineering, Czech Technical University in Prague, Zikova 1, 160 00 Prague 6, Czech Republic
[3] Faculty of Biomedical Engineering, Czech Technical University in Prague, Sítná sq. 3105, 272 01 Kladno, Czech Republic
[4] Institute for Materials Research (IMO), Hasselt University, Wetenschapspark 1, 3590 Diepenbeek, Belgium
[5] J. Heyrovský Institute of Physical Chemistry, AS CR, v.v.i., Dolejškova 3, 182 23 Prague 8, Czech Republic
[6] Institute of Organic Chemistry and Biochemistry AS CR, v.v.i., Flemingovo námìstí 2, 166 10 Prague, Czech Republic
[7] Institute of Physics, Academy of Sciences Czech Republic v.v.i, Cukrovarnická 10, 162 00 Prague 6, Czech Republic
[8] Nuclear Physics Institute Academy of Sciences of the Czech Republic v.v.i, 250 68 Rez near Prague, Czech Republic

Received 28 May 2013 / Received in final form 24 August 2013
Published online (Inserted Later) – © EDP Sciences, Società Italiana di Fisica, Springer-Verlag 2013

Abstract. The resistivity of boron doped polycrystalline diamond films changes with boron content in a very complex way with many unclear factors. From the large number of parameters affecting boron doped polycrystalline diamond film's conductivity we focused on the role of boron atoms inside diamond grains in terms of boron contribution to the continuum of diamond electronic states. Using a combination of theoretical and experimental techniques (plane-wave Density Functional Theory, Neutron Depth Profiling, resistivity and Hall effect measurements, Atomic Force Microscopy and Raman spectroscopy) we studied a wide range of B defect parameters – the boron concentration, location, structure, free hole concentration and mobility. The main goal and novelty of our work was to find the influence of B defects (structure, interactions, charge localisation and spins) in highly B-doped diamonds – close or above the metal-insulator transition – on the complex material charge transport mechanisms.

1 Introduction

Diamond is known to be a remarkable material due to its particularly attractive properties combining chemical resistance, optical transparency, thermal conductivity, high bio-inertness and electrochemical properties [1–6]. There is considerable interest in diamond as a future material for electronic applications (high power-high temperature electronics, radiation-hard electronics, radiation detectors, and vacuum electronics).

Diamond is generally recognized as an insulating material. Once successfully doped it is a wide-bandgap semiconductor material with an excellent application potential due to the unique combination of its physical and electronic properties. The small boron (B) atom seems to be the only efficient dopant atom in diamond, which can be incorporated with high reproducibility and in high enough concentrations to be useful for electronic devices [7,8]. By adding B species to the precursor gas mixture chemical vapour deposition (CVD) [6] production of boron doped diamond (BDD) films is accomplished reproducible [6,9,10]. B in a diamond lattice acts as an electron acceptor giving the diamond p-type semiconducting properties. The acceptor level introduced by B is quite deep – 0.37 eV from the top of the valence band [6,7]. At low temperatures or at B concentrations of 10^{17} cm^{-3} conduction occurs through holes in the valence band contributed by ionised substitutional B. At higher doping levels, conduction occurs by nearest-neighbour and variable range hopping of holes between ionised B sites. Further addition of B completely changes the type of electrical conductivity in diamond layers [11,12] – high B concentrations (above 3×10^{20} cm^{-3}) typically result in a conductive system with electrical properties comparable to metallic materials. Even superconductivity at 4 K was reported by Ekimov et al. [7] in heavily B-doped diamond.

Here we studied the conductivity of BDD polycrystalline films which were synthesized by microwave plasma enhanced chemical vapour deposition (MW PECVD) on quartz substrates. Conductivity is a complex physical quantity and in the case of BDD films there are many parameters that influence charge transport [4–6,12–18]: (i) size of the diamond grains – conductance of BDD films

[a] e-mail: krat@fzu.cz

Investigation of nitrogen content of nano-crystalline diamond layers (NCD)

Neutron Physics Laboratory - Nuclear analytical methods with neutrons

Andy Taylor

Proposal ID

67

CANAM report – Proposal ID: 67

Investigation of nitrogen content of nano-crystalline diamond layers (NCD)

Pulsed microwave plasma enhanced chemical vapour deposition apparatus with linear antenna delivery system using $CO_2/CH_4/H_2$ gas chemistries is a versatile system that allows large area growth of nanocrystalline diamond (NCD) at low temperatures [1]. However, one of the drawbacks of the system in comparison with conventional resonance cavity MW CVD systems is lower growth rates. High growth rate is essential for many commercial applications. To overcome this problem while maintaining low temperature, we investigated the catalytic effect of nitrogen in the gas phase that is known to enhance the growth rate [2]. Nitrogen concentrations were varied from 0.1 to 5% in the gas phase and the effect of this addition on the growth rate was investigated. N content of the grown NCD films were analysed using neutron depth profiling (NDP) and compared with the morphology, grain size, structure, and quality (sp^3/sp^2 ratio) characterized by scanning electron microscopy (SEM), atomic force microscopy (AFM), X-ray diffraction, and Raman spectroscopy.

The complex gas chemistry induced by nitrogen addition led to two effects. The growth rate of the diamond films indeed increased when nitrogen was added. However, upon increasing the nitrogen concentration, the morphology changed significantly. For high N concentrations the NCD morphology resembles highly N-doped ultrananocrystalline diamond (UNCD) films grown in Ar rich atmospheres [3] in terms of clustering nano-grains into larger ordered clusters and is significantly distinguished from so called “cauliflower” nanodiamond which has been prepared in N-containing resonance cavity plasmas. Furthermore, the sp^3/sp^2 ratio and diamond Raman peak remained unchanged, when compared with samples prepared without nitrogen at the same growth conditions.

NPD confirmed the presence of N at levels greater than that of background boron content. Also confirmed was the necessity to “dope” the chamber as the first two attempts at N doping showed no N content according to NDP. It can be supposed that this was due to losses of N to the chamber walls (i.e. they require “doping” before N is incorporated into the crystal lattice).

Further work is planned for the near future to further investigate N incorporation with the aim of creation of optically active NV centers which can act as near surface sensors.

[1] A. Taylor et al: Diamond & Related Materials 20 (2011) 613-615
[2] S. Dunst, et al: Appl. Phys. Lett. 94, 224101 (2009)
[3] D. Gruen: MRS BULLETIN 26, 10, 771-776 (OCT 2001)

NDP Experiment Time Application

Neutron Physics Laboratory - Nuclear analytical methods with neutrons

Xin Yang

Proposal ID

66

There are two samples have been measured by NDP, a natural boron coating on the silicon matrix sample and a LiF(natural Li) coating on the silicon matrix.

The measurement was performed in UHV chamber using the Hamamatsu detectors (8 × 8 mm^2) and distance from the sample 40 mm. The beam intensity was around $10^7/(cm^2s)$. The evaluation is based on the comparison with the B standard NDP pattern

The NDP spectrum are shown in Fig.1.

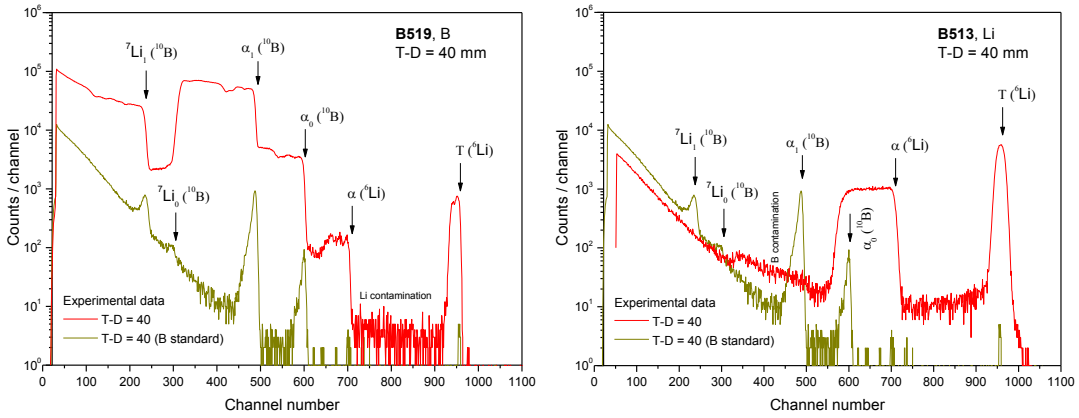

Fig 1. The spectrum of samples

The B sample is very inhomogeneous and contaminated by Li. The LiF sample looks relatively OK with a smooth alpha line platform and also be contaminated by B.

Profile results are shown in Fig 2.

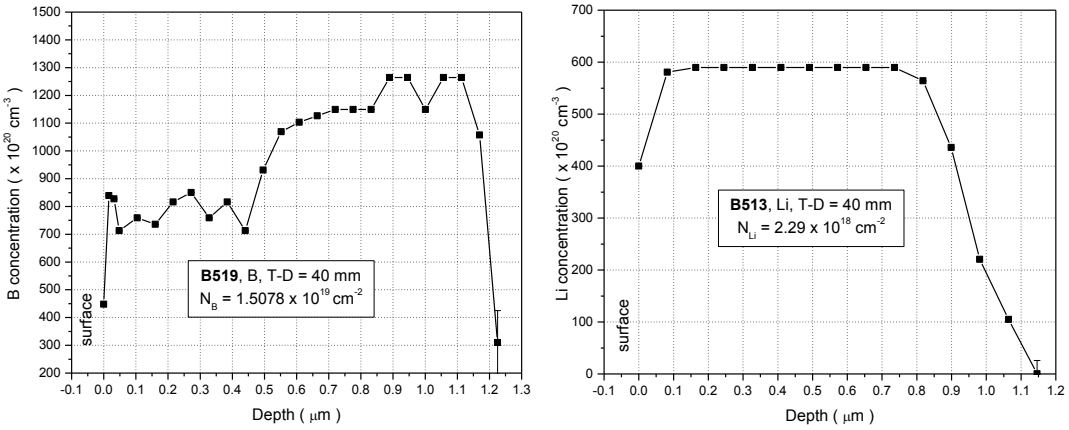

Fig 2. Profile of ^{10}B and ^7Li

The research has been conducted at the CANAM (Center of Accelerators and Nuclear Analytical Methods LM2011019) infrastructure with a funding from the Ministry of Education, Youth and Sports of the Czech Republic.

Study of the 17O(n,) reaction via the ANC method

Laboratory of Cyclotron and Fast Neutron Generators

Livio Lamia

Proposal ID

61

Study of the $^{17}O(n,\alpha)$ reaction via the ANC method: FINAL REPORT

L. Lamia[1,2], C. Spitaleri[1,2], L. Guardo[1,2], M. Gulino[1,2], V. Burjan[3], V. Kroha[3], J. Mrazek[3], M. La Cognata[1], R. G. Pizzone[1], S. Romano[1,2]

1- INFN-LNS, Catania, ITALY
2- University of Catania, ITALY
3- NPI ASCR, Rez, Czech REP.

The $^{17}O(n,\alpha)^{14}C$ reaction plays a key role in several astrophysical scenario such as Inhomogeneous Big Bang Nucleosynthesis (IBBN) or heavy-element production during the weak component of the s-process. Thus, its reaction rate must be known in the energy region of interest for astrophysics, going from few keV's up to about 400 keV. At such energies, the intermediate $^{17}O+n \rightarrow ^{18}O$ nucleus presents four excited levels (8038, 8125, 8213, and 8282 keV's) affecting the magnitude of the $^{17}O+n$ cross section. For such a reason, in an earlier experiment, the $^{17}O(n,\alpha)^{14}C$ reaction has been studied by means of the indirect method of the Trojan Horse (THM, Spitaleri et al. 2011) applied to the quasi-free $^{2}H(^{17}O,\alpha^{14}C)p$ reaction. This investigation allowed us to study the $^{17}O(n,\alpha)^{14}C$ at astrophysical energies, thus validating once again the deuteron quasi-free break-up as source of virtual neutrons (Gulino et al., 2013). Because of the lack of spectroscopic information about the 8125 keV ^{18}Oresonant level, we have performed a devoted experiment at NPI ASCR Rez, by studying the emitted proton spectra of the $^{17}O(d,p)$ reaction.

For the experiment, we have used a high intensity 16.4 MeV deuteron beam of U120M cyclotron of NPI ASCR Rez, impinging on a 150 mbar ^{17}O gas target. We have used a well equipped detection setup having five telescope detectors placed at 23°, 33°, 43°, 53° and 63° degrees (in the lab.), and three telescope monitors at 20°, 30° and 40° degrees. Additional data of a previous experiment will allow us to cover the angles 17°, 27° and 37°, thus allowing a large covering of the experimentally studied center-of-mass angular region. Regarding the collected data, we were able to collect a good statistics (for the eight new angles and better by a factor 2). The data evaluation, as well as careful evaluation of the uncertainties, is currently under process in off-line analysis. For our purposes, we have also used an ^{15}N gas target for calibration and estimation of parasitic effects and, in the last day, a solid mylar target to measure beam energy and to compensate/identify small beam angular deviations. All the procedure described above has been performed in about 7 days and involved 5 researchers of NPI ASCR Rez and 4 researchers of Univeristy of Catania-INFN LNS.

Determination of boron concentration profile in nanocrystalline diamond films of variable grain size

Neutron Physics Laboratory - Nuclear analytical methods with neutrons

Pavel Hubík

Proposal ID

62

Experiment report on "Determination of boron concentration profile in nanocrystalline diamond films of variable grain size" (ID 62, proposer Pavel Hubík)

The proposed NDP measurement of boron concentration in thin films of nanocrystalline diamond was carried out. Thin film boron standard with boron concentration of 1.42×10^{16} cm^{-2} was used as a reference. Estimated depth resolution in the performed measurement, 20-30 nm, was comparable to the width of the doped diamond films (50-120 nm as obtained from optical measurements), therefore the determination of profiles was not possible. Consequently, the main output of the NDP measurement was the surface (area) concentration of boron in each sample studied. The obtained concentrations were in the range of $(0.2\text{-}1.1) \times 10^{15}$ cm^{-2}. These values were recalculated, using the thickness values, to bulk boron concentrations. The resulting bulk concentrations ranged from 4×10^{19} cm^{-3} to 9×10^{19} cm^{-3}. This concentration range is significantly narrower than that obtained in the previous set of the boron-doped nanocrystalline diamond (BNCD) thin films prepared by the same technology. At the same time, this new set did not reveal a monotonic (increasing) dependence of the boron concentration on the mean (Heyn) grain size, which was found before. Such an observation has led us to the conclusion that the hypothesis that the preferential orientation of large BNCD grains causes different boron incorporation cannot be proved. This conclusion was also supported by X-ray diffraction measurement performed subsequently, in which no well-defined preferential orientation was found in any of the samples studied.

On the other hand, a relatively narrow range of the boron concentrations in the new set of samples (scatter by a factor of about 2 only) is favorable for the original intent of the study, i.e. investigation of the transport mechanism in BNCD as a function of the grain size. Research into this topic is currently conducted by means of the magnetotransport measurement in a wide temperature range. The measurements are expected to be finished within about 3 months. Afterwards, using results of these experiments and the reported CANAM project, we will prepare a journal publication.

Radiation Hardness of the ATLAS-HEC Cold Electronics

Laboratory of Cyclotron and Fast Neutron Generators

Milan Štefánik

Proposal ID

59

Final Report

Neutron irradiation test has been performed to evaluate the limits of the current readout electronics under HL-LHC conditions. The GaAs ASIC which comprises the heart of the readout electronics has been exposed to neutron radiation with fluences up to ten times the total expected fluences for ten years of running of the HL-LHC. Neutron tests were performed at the NPI in Rez, where a 36 MeV proton beam is directed on a thick heavy water target to produce neutrons of broad spectrum up to 32 MeV.

In the neutron test, the setup was as follow: 16 equidistant slots with distances of 1.7 cm between adjacent board centers have been equipped and placed in front of the 3 mm steel plate enclosing the heavy-water target. The alignment was done after the mounting the target to the beam-line of ischochronous cyclotron U-120M operated in negative ion-mode of acceleration. Slots were equipped with the BB96 GaAs ASICs, two selected slots were equipped with the radiation diodes, one slot with activation foils, and the remaining slots with test structures for the HEC power supplies. The neutron flux profile has been measured with sheets of EBT2 radiation film placed for approx. 2 hours at a reduced machine current of about 1 μA between each two slots.

In the neutron test triangular voltage pulses similar to the ionization currents in the LAr gaps in ATLAS have been also applied over the 40 m cables at the BB96 ASICs and both the input and the output pulse have been measured with an oscilloscope. These measurements were done alternatingly with the scattering parameter measurements and provide another way of studying the performance of the electronics.

The irradiation tests of the current readout electronics of the Hadronic Endcap Calorimeter of ATLAS with neutrons with fluence levels exceeding those relevant for the high luminosity upgrade of the LHC have been successfully performed; data processing is in progress.

Radiation Hardness of Si Pixel Chips and Components for ALICE Inner Tracker System Upgrade Project

Laboratory of Cyclotron and Fast Neutron Generators

Jozef Ferencei

Proposal ID

60

CANAM project:
"Radiation Hardness of Si Pixel Chips and Components for ALICE Inner Tracker System Upgrade

During the course of 2013 year the following measurements were made in U-120M cyclotron of Nuclear Physics Institute in the framework of CANAM project Nr. 60 "Radiation Hardness of Si Pixel Chips and Components for ALICE Inner Tracker System Upgrade":

1. Series of measurements to determine Single Event Upset (SEU) probability for SRAM memories in 180 nm technology from TowerJazz foundry in Israel, foreseen for mass production of silicon pixel chips for ALICE inner tracker system upgrade. Results confirmed the acceptable SEU rate at the level of 10^{-13} cm^2bit^{-1} causing rather tolerable data corruption (~10^{-9} bit^{-1} for central most affected chip) with no necessity for special expensive protections. This is important verification of technology suitability for production of monolithic active pixel sensors (MAPS) with on-chip integrated electronics. Measurements at U-120M cyclotron together with the ones carried at higher energies in Paul Scherer Institute in Villigen, Switzerland are part of the published "*Technical Design Report for the Upgrade of the ALICE Tracking System*", CERN-LHCC-2013-024, ALICE-TDR-017, which is available at CERN document server using the following URL: http://cds.cern.ch/record/1625842/files/ALICE-TDR-017.pdf?version=3 (pages 38-39). This document was submitted to 116th meeting of LHC Experiments Committee held on 4.12.2013 for endorsement. Investigations will continue using higher beam currents to study Single Event Latch-ups, i.e. the functional failure studies.
2. After careful selection procedure made in CERN the suitable fast (up to 6 Gbit/s) signal cable candidate 30 AWG Micro Twinax Cable from Samtec Company was chosen. Proton irradiation up to the total ionization dose of 1 Mrad was made in U-120 M cyclotron. The cable was shipped back to CERN, where measurements using fast oscilloscope with specialized pseudo random bit sequence generator confirmed unchanged bit error rate probability. This activity will continue for the laminated version of same type of cable, which is more compact w.r.t. non-laminated version.
3. For ALICE Inner Tracker System upgrade project the field-programmable gate arrays (FPGA) are foreseen to cope with expected enormous data volume (up to 30 Gbit/sec). As these FPGA will be located in LHC accelerator radiation environment, the unavoidable selection procedure of radiation hard commercially available FPGA was initiated. To precede with this complex task two PhD students from Faculty of information technology Czech technical university in Prague joined our group. First test measurements using Xilinx Spartan XC3S200 FPGA were already made. The detailed radiation hardness studies of modern Flash FPGA (expected to be more radiation hard) SmartFusion2 from Microsemi Company are in preparation.

Understanding the structure of transparent zirconia glasses

Neutron Physics Laboratory - Neutron diffraction

Gennady Kopitsa

Proposal ID

23

EXPERIMENTAL REPORT

Title. Understanding the structure of transparent zirconia glasses

Objectives. Transparent amorphous oxide glasses are considered to be very promising materials for photochromic devices, catalytic systems, chemical sensors, etc. These materials are also proposed as matrices for thermally stable luminescent nanocomposites (containing either II-VI semiconductor nanoparticles of rare-earth compounds) and non-linear optics devices, especially lasers. Up to now, amorphous glasses were mostly made from silica and due to this reason the range of their possible applications was considerably limited. Recently we've succeeded in development of sol-gel technique of transparent zirconia glasses possessing very high surface area (up to 400 m^2/g). The method proposed doesn't include supercritical drying stage, so it's truly low cost and efficient.
Thus, the aim of the present study was to investigate for the first time the mesostructure of transparent porous zirconia glasses formed by sol-gel technique and to elucidate reliably the possibility of fine tuning of their characteristics. This task is supposed to be solved by using both USANS, SANS and complementary methods (TEM, XRD, TGA/DTA/DSC, etc.).

Experiment
1. Samples. Six series of the samples of zirconia glasses prepared by slow hydrolysis of zirconium propoxide in the presence of water, nitric and hydrochloric acids, isopropanol, dimethylformamide, acetylacetone etc. were studied.
2. USANS. The HR-SANS experiment was performed at the double-crystal diffractometer MAUD of LVR-15 research reactor in Prague (Czech Republic), which using neutrons with the wavelengths $\lambda = 2.09$ Å ($\Delta\lambda/\lambda = 0.18$). The range of momentum transfer $2.5\cdot10^{-4} < q < 4\cdot10^{-3}$ $Å^{-1}$. All measurements were made at room temperature.

Achievements and Main Results. Figure 1 shows the experimental $d\Sigma(q)/d\Omega$ *vs.* q curves for zirconia glasses prepared by slow hydrolysis of zirconium propoxide in isopropanol-based media with various water content at room temperature (Fig. 1a) and $T = 0^oC$ (Fig. 1b). These data clearly demonstrate that small-angle scattering for $ZrO_2\times xH_2O$ grasses depends upon both water content and the temperature of synthesis.

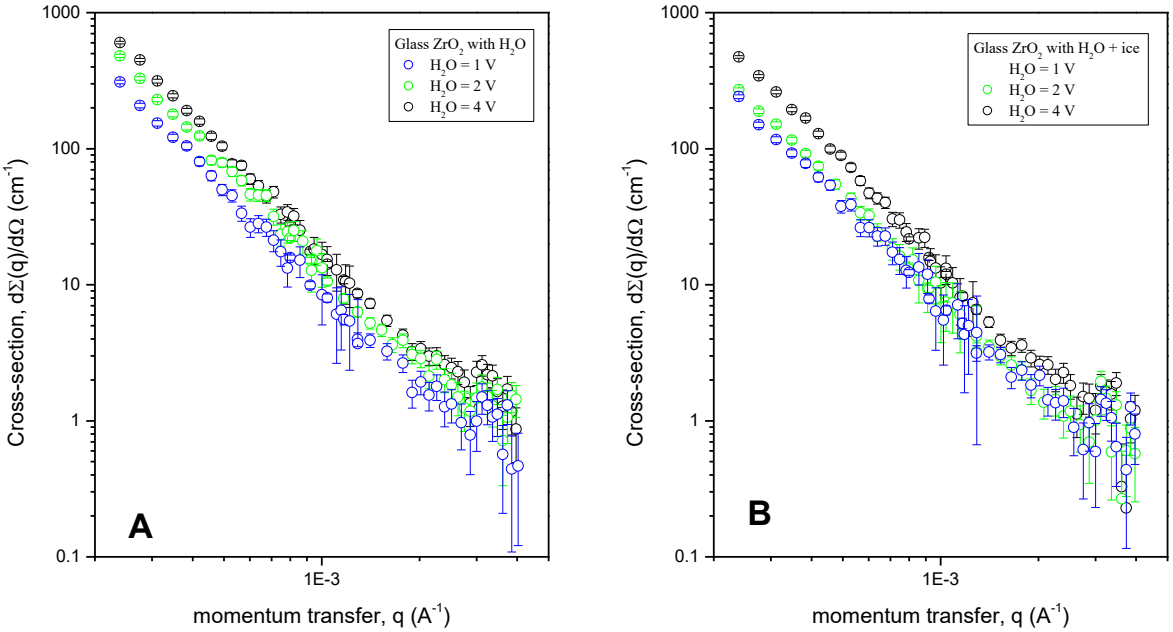

Figure 1. Experimental $d\Sigma(q)/d\Omega$ *vs.* q curves for zirconia glasses

The treatment of USANS data for samples of zirconia glasses prepared by slow hydrolysis of zirconium propoxide in the presence of water, nitric and hydrochloric acids, isopropanol, dimethylformamide, acetylacetone etc. and interpretation of all the data obtained is still in progress.

Inner structure of the basic element of large sintered artificial opals

Neutron Physics Laboratory - Neutron diffraction

Gennady Kopitsa

Proposal ID

25

EXPERIMENTAL REPORT

Title. Inner structure of large sintered artificial opals

Objectives. The experiment aims the structural characterization of new material made on the base of silicon dioxide spheres synthesized by modified Stober method. The diameter spheres is varied from 320 nm to 2200 nm in different samples with monodispersity better than 5%. In previous SAS experiments we determined that this spheres have initial particles with size 7-10 nm. It is obtained from SEM at higher contrast and magnification demonstrates the edge of the cross-section of the particle having the several undeformed secondary particles of size of order 60 nm of quasi-sphere, or oval shapes[1]. The experiment goal was to uniquely determine by non-destructive method (HR-SANS) if there are secondary particles.

Experiment

1. Samples. Silica particles were prepared using the modified Stöber method by the tetraethylorthosilicate (TEOS) hydrolysis reaction in aqueous-alcoholic solution in the presence of ammonium hydroxide (50% vol. ethanol, 1.0 M ammonium).

2. Ultra small-angle neutron scattering. The HR-SANS experiment was performed at the double-crystal diffractometer MAUD of LVR-15 research reactor in Prague (Czech Republic), which using neutrons with the wavelengths $\lambda = 2.09$ nm ($\Delta\lambda/\lambda = 0.18$). The range of momentum transfer $2\times10^{-4} < Q < 2\times10^{-2}$ A^{-1}.
All measurements were made at room temperature.

Achievements and Main Results. The inner structure was studied by USANS method. There are scattering curves in double logarithmic scale on the figure 1. These data clearly demonstrate that small-angle scattering depends on sphere diameters.

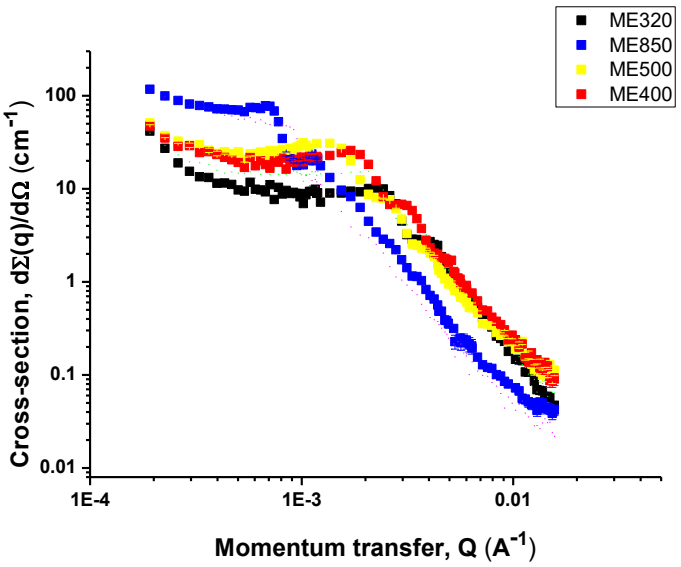

Fig. 1 The HR-SANS cross section $d\Sigma(q)/d\Omega$ for the samples of silica particles with different diameters (■ - 320, ■ - 400, ■ - 500, ■ – 850 nm)

The treatment of SANS data for samples of artificial opal and interpretation of all the obtained data is still in progress.

References

[1] V.M. Masalov et. al. Direct observation of the shell-like structure of SiO2 particles synthesized by the multistage Stöber method. NANO: Brief Reports and Reviews Vol. 8, No. 4 (2013)

Neutron based analytical methods for investigation of carbon based materials

Neutron Physics Laboratory - Nuclear analytical methods with neutrons

Zdenek Sofer

Proposal ID

19

Project Title: **Neutron based analytical methods for investigation of carbon based materials**

Proposer: **Zdenek Sofer (zdenek.sofer@vscht.cz)**

Lab: **Neutron Physics Laboratory - Nuclear analytical methods with neutrons**

NAA method was used for the evaluation of impurities concentration in graphene and graphene oxide which were prepared by various methods. Metallic impurities have significant effect on electrochemical properties and subsequent applications of carbon nanomaterials. Such as in case of carbon nanotubes (CNT) the electrochemical properties are dominated by electrochemical properties of metallic impurities. High purity graphite was used in order to avoid introduction of impurities to the starting material. Starting graphite oxides were prepared by Brodie, Staudenmaier, Hofmann and Hummers methods. Various methods led to the introduction of impurities related to the chemicals used for oxidation. High concentration of manganese was observed in graphene oxide and also graphite prepared by Hummers method. In all graphite oxides and graphenes high concentrations of alkali metals (sodium and potassium) were measured. The increase of impurities concentration was observed during the whole process (oxidation of graphite and subsequent reduction). In this case graphene oxides acted as a sorption material and they concentrated various metals. Their concentration was further increased during the reduction of graphene oxide (chemical and thermal reduction). During the reduction process oxygen functional groups are removed and impurities are concentrated within graphene. Other methods like PIXE and ICP-OES were used for the comparison of results obtained by NAA. NAA method is the most suitable for elements with high cross section of thermal neutrons. PIXE has a very low sensitivity for light elements. For ICP-OES analysis the sample must be dissolved and these procedures often introduce significant deviations in the analysis results.

The obtained concentrations of metallic impurities were correlated with the results of ICP-OES (which gave lover results) and PIXE. Based on the analytical results the electrochemical measurement (cyclic voltammetry) with various redox probes was performed. The redox probes with high sensitivity towards metallic impurities were tested (like hydrogensulphide ions and cumene hydroperoxide) and also standard redox probe ($[Fe(CN)_6]^{3-/4-}$) was used for calculation of heterogeneous electron transfer (HET) rate.

Obtained results are evaluated and they will be published in impacted journal within six months.

Structure of new silica, alumina, and zirconia aerogels with unusual properties

Neutron Physics Laboratory - Neutron diffraction

Gennady Kopitsa

Proposal ID

22

EXPERIMENTAL REPORT

Title. Structure of new silica, alumina and zirconia aerogels with unusual properties

Objectives. Aerogels are unique mesoporous materials having more than 90% porosity. The structure of aerogels corresponds to ramified network of nanoparticles clusterswith 10–100 nm pores. Extremely high porosity and low density of aerogels results in their low thermal conductivity and high thermal stability – up to 1200°C. These materials are excellent heat and sound insulators and have proved to be effective heterogeneous catalysts. Nanomaterials based on noble metal or intermetallic nanoparticles introduced in aerogel matrices are considered also as hydrogen storage materials.
The aim of the present study is to investigate the mesostructure of SiO2, Al2O3, ZrO2 aerogels formed by the novel supercritical drying technique and to gain information on their fractal characteristic, aggregate structure, porosity, etc. This task is supposed to be solved by using complementary methods (TEM, XRD, TGA/DTA/DSC, etc.).

Experiment
1. Samples. Series of the samples of SiO2, Al2O3, ZrO2 aerogels prepared by the novel technique of supercritical drying gel using different solvents like ethanol, hexafluoruisopropanol, diethyl ether and methyl tret-buthyl ether.
2. USANS. The HR-SANS experiment was performed at the double-crystal diffractometer MAUD of LVR-15 research reactor in Prague (Czech Republic), which using neutrons with the wavelengths $\lambda = 2.09$ Å ($\Delta\lambda/\lambda = 0.18$). The range of momentum transfer $2.5\cdot10^{-4} < q < 1.2\cdot10^{-2}$ Å^{-1}. All measurements were made at room temperature.

Achievements and Main Results. Mesostructure of aerogels was studied by USANS and SANS methods. Figure 1 shows the experimental $d\Sigma(q)/d\Omega$ *vs.* q curves for aerogels based on zirconia prepared by using different solvents (ethanol(EtOH), hexafluoroisopropanol(HFIP) and diethyl ether(Et2O)). These data clearly demonstrate that small-angle scattering depends on using solvents.

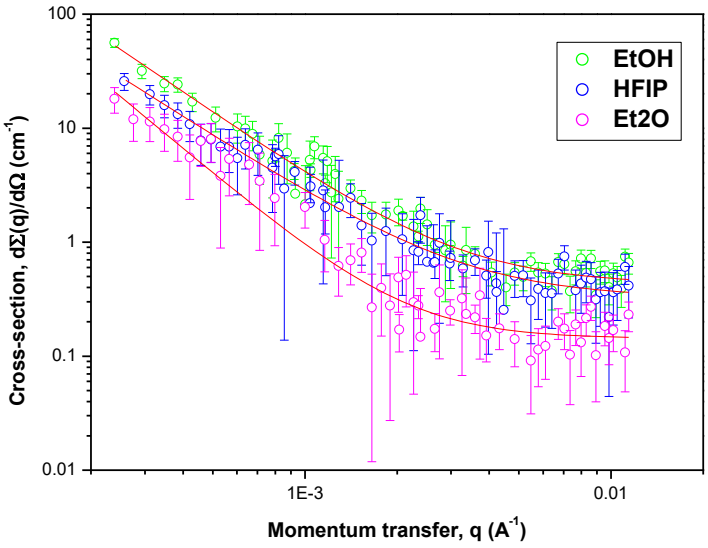

Figure 1. Experimental $d\Sigma(q)/d\Omega$ *vs.* q curves for aerogels based on zirconia with using different solvents (ethanol(EtOH), hexafluoroisopropanol(HFIP) and diethyl ether(Et2O)).

It is clearly seen that $d\Sigma(q)/d\Omega$ for all samples satisfies the power law q^{-n}. For aerogels prepared with using ethanol(EtOH) and hexafluoroisopropanol (HFIP) solvents the exponent n values are equal 1.7 and 1.85. It means that the scattering from these aerogels occurs on the volume fractals with the dimensions $D_V = n + 1 \approx 2.7$ and 2.85, respectively. In the case of the aerogel prepared with using diethyl ether (Et2O) solvent the exponent $n \approx 2.3$. This corresponds to the scattering from the fractal surface with the dimension $D_s = 6 - (n+1) = 2.7$.

The treatment of SANS data for samples of SiO2, Al2O3, ZrO2 aerogels and interpretation of all the obtained data is still in progress.

Effect of high LET radiation on specific interaction of proteins with DNA.

Laboratory of Cyclotron and Fast Neutron Generators

Marie Davidkova

Proposal ID

21

Průběžná zpráva o realizaci projektu za rok 2012

Projekt je řešen jako příspěvek řešitelského týmu k mezinárodnímu projektu COST MP1002 "Nano-scale insights in ion beam cancer therapy (Nano-IBCT, Nano-aspekty iontové terapie nádorů)“. Řešitelská laboratoř je součástí pracovní skupiny WG5 Radiobiologické efekty (detekce dvojných zlomů DNA, predikce a buněčné projevy poškození). Cílem projektu je určit jakým způsobem ovlivňuje radiační poškození reparačních proteinů rychlost a správnost reparačních mechanismů v buňkách.

Ozařování biologických vzorků na urychlovačích v ÚJF v Řeži, cyklotron U120M a tandetron, je specifické díky energiím dostupných nabitých částic. Maximální energie protonů na cyklotronu U120M je přibližně 34 MeV, na tandetronu 6 MeV. Dosah těchto iontů ve vodě je pouze několik desítek μm až mm (protony 6 MeV mají ve vodě dosah přibližně 0,5 mm, 34 MeV 11 mm), proto je třeba pracovat s tenkými vrstvičkami vzorků.

Bylo navrženo a testováno několik možných řešení:

a) Prototypové plastové nebo kovové kroužky držící velmi tenkou Mylar folii vyrobené v ODZ ÚJF
b) Sterilní Petriho misky s kruhovým otvorem ve dně, na které je nalepeno krycí mikroskopické sklíčko
c) Komerčně dostupné plastové misky, u kterých je dno a případně i víčko nahrazeno Mylar folií (firma Chemplex, USA).

Navržená řešení byly testovány během ozařování na cyklotronu U120M. Pro další experimenty s neonatálními dermálními fibroblasty se jeví jako nejvhodnější řešení varianta c. Pro experimenty realizované ve spolupráci s kolegy z Biofyzikálního ústavu AV ČR v Brně, kdy byly buňky analyzovány metodou FISH (fluorescenční in situ hybridizace) se jeví výhodnější uspořádání v Petriho miskách (varianta b). Buňky rostou přímo na mikroskopickém sklíčku, po ozáření jsou dále zpracovány a analyzovány fluorescenčním mikroskopem. DNA ve vodných roztocích jsou ozařovány v úzkých plastových mikrozkumavkách.

Podíl přímého a nepřímého účinku ve stopách protonů byl studován s použitím DNA plasmidů pBR322 ve vodných roztocích. Vzorky obsahovaly různé koncentrace sloučenin vychytávající hydroxylové radikály (kumarin-3-karboxylová kyselina, dimethylsulfoxid nebo glycylglycin). Metodou agarózové elektroforézy byly stanoveny výtěžky jednoduchých a dvojných zlomů DNA. V závislosti na koncentraci vychytávače lze odhadnout podíl přímého poškození DNA a příspěvek nepřímého poškození prostřednictvím OH radikálů. Tyto informace budou velmi zajímavým výstupem projektu, zvláště pokud získáme větší rozsah různých iontů a energií.

Radiační poškození proteinů bylo studováno u restrikčních enzymů HindIII a PvuII. Enzymy ozářené rostoucími dávkami záření byly inkubovány s pCDNA3 plasmidy a vzorky byly poté analyzovány metodou agarózové elektroforézy. Funkční enzymy rozpoznávají specifickou sekvenci bazí a v tomto místě DNA štěpí. Proteiny poškozené zářením postupně ztrácejí schopnost rozpoznat a štěpit DNA. Bylo sledováno snižování aktivity enzymů s rostoucí dávkou záření.

V prvním roce řešení projektu nebylo plánováno získání výsledků pro buněčné kultury. V rámci přípravy byly nicméně připraveny metodiky pro realizaci experimentů, potřebné laboratorní uspořádání a byly realizovány první pilotní experimenty. Křivky přežití byly měřeny pro konfluentní neonatální fibroblasty pěstované na 2,5 μm Mylar foliích a ozářených rostoucími dávkami gama záření a 15 a 30MeV protonů. V ozářených vzorcích bylo stanoveno přežití buněk a četnost výskytu mikrojader. Experimenty budou zopakovány, doplněny a analyzovány. Ve spolupráci s Biofyzikálním ústavem AV ČR, v.v.i. proběhly i první experimenty zaměřené na reparaci DSB v neonatálních fibroblastech v závislosti na struktuře chromatinu v buněčném jádru.

Characterization of impurities in carbon nanomaterials

Laboratory of Tandetron

Zdenek Sofer

Proposal ID

16

Project Title: **Characterization of impurities in carbon nanomaterials**
Proposer: **Zdenek Sofer** (zdenek.sofer@vscht.cz)
Lab: **Laboratory of Tandetron**

Measurements in Tandetron laboratory were used for RBS/ERDA and also PIXE analysis. The RBS method was used for the characterization of carbon nanomaterials (measurement of C/O/H ratio) and also semiconductor thin films implanted with rare earths and transition metals (GaN and ZnO).

The deep concentration profiles and total amount of Gd ions with ZnO substrates were measured. The RBS measurement was also used to evaluate the damage induced by ion implantation and further recovery of layered structure by annealing in various atmospheres. The ZnO layers were also characterized by Raman spectroscopy, SQUID magnetometry and AFM measurements. Obtained results were correlated with data from RBS. The ferromagnetism was observed only for as gadolinium implanted ZnO substrates and subsequent annealing led to paramagnetic behavior. From this results we can conclude that in the case of ZnO the exotic ferromagnetism is correlated to the presence of ion implantation induced defects and possible presence of gadolinium nanoclusters. RBS measurements were used also for the characterization of GaN thin films implanted with various rare earths elements (Ho, Tb and Tm). The RBS method was used to measure concentration profiles and for the estimation of total dose of implanted ions. The partial recovery of layered structure was observed after high temperature treatment of the layer. Formation of defects on the layer surface was observed for the doses over $1x10^{16}$ at.cm^{-2} (at 200 keV energy).

The RBS/ERDA method was used for the measurement of C/H/O ratios in graphene based materials. Results were correlated to the data obtained by elemental combustion analysis. In the case of RBS higher C/O ratio was observed. This is related to the partial decomposition of graphene and further removed oxygen functionalities due to the interaction with ion beam used for measurements. The PIXE and PIGE methods were used to measure heavy and light elements concentration, respectively. The concentration of boron was correlated with results obtained by PG-NAA. The concentrations of metallic impurities obtained by PIXE were correlated to the concentrations obtained by ICP-OES and NAA. In comparison to ICP-OES method, PIXE had advantages related to easier sample preparation for analysis. For the ICP-OES the sample must be decomposed and transferred to the solution by combustion and acid digestion. This procedure is not sufficiently effective and lover concentrations of metallic impurities are often observed. Obtained results were compared to data obtained by ICP-OES and NAA and subsequently correlated to the electrochemical characterizations. The results of PIXE and RBS/ERDA measurement of graphene will be published within six months.

Published results:

A. Mackova, P. Malinský, Z. Sofer, P. Šimek, D. Sedmidubský, M. Mikulics: A Study of the Structural properties of GaN implanted by various rare-earth ions, Nuclear Instruments and Methods in Physics Research Section B: Beam Interactions with Materials and Atoms, 307 (2013) 446-451.

Mackova, P. Malinský, Z. Sofer, P. Šimek, D. Sedmidubský, M. Mikulics, R. A. Wilhelm: A Study of the Structural and Magnetic Properties of ZnO Implanted by Gd Ions, Nuclear Instruments and Methods in Physics Research Section B: Beam Interactions with Materials and Atoms, accepted.

RNAA for selenium determination in wheat samples

Neutron Physics Laboratory - Nuclear analytical methods with neutrons

Catarina Galinha

Proposal ID

15

Background

Cereals are an important component on human nutrition and are considered a good source of proteins and one of the major dietary sources of selenium (Se) when it is available at soil. Different methods of selenium supplementation were used. Foliar addition in two different growth stages (booting and grain filling), the addition of selenium to soil prior to sowing and selenium enriched seeds. Selenium in wheat samples were analysed by INAA (Instrumental Nuclear Activation Analysis), and CINAA (cyclic INAA) on the fast pneumatic system (SIPRA) available at the Portuguese Nuclear Reactor (RPI), using respectively ^{75}Se and ^{77m}Se. The values of selenium were below the detection limit, and values could not be determined.

Experimental

Samples from soil supplementation, reference materials, blank ampoules and standards were irradiated in the LVR-15 light-water reactor for 20 h. The irradiated samples were allowed to cool for 1 month. After separation the samples were measured with a well-type HPGe detector for 2 h. The Se separation yield was determined through reactivation of a carrier by short-time irradiation (30 s) in a pneumatic facility, and counting of the ^{77m}Se radioisotope with a coaxial HPGe detector. For quantification of Se contents in the samples an irradiated liquid ^{75}Se standard was used.

Results and Discussion

The experiment was extremely well executed. Due to a very high yield and selectivity of the Se chemical separation RNAA is a very suitable method to achieve Se in samples where this element has very low concentrations. Table 1 resumes the values determined within this study.

Table 1. Selenium concentrations attained for the analyzed samples.

Type of Sample	Sample Code	[Se] (mg/kg)
Bread Wheat	JBrancoFoliar	73
Bread Wheat	JBranco	43
Bread Wheat	RBranco	68
Bread Wheat	SOJ4SA3	9
Bread Wheat	SOJ4SAKI2	10
Bread Wheat	SOJ4SIKI2	12
Bread Wheat	SOJ20SA1	23
Bread Wheat	SOJ20SA2	57
Bread Wheat	SOJ20SI3	19
Bread Wheat	SOJ100SA1	126
Bread Wheat	SOJ100SA2	28
Bread Wheat	SOJ100SA3	98
Bread Wheat	SOJ100SAKI1	791
Bread Wheat	SOJ100SAKI2	530
Bread Wheat	SOJ100SAKI3	280

Type of Sample	Sample Code	[Se] (mg/kg)
Soil	SoloGenerico	92
Durum Wheat	MBrancoFoliar	167
Durum Wheat	MBranco	44
Durum Wheat	CBranco	34
Durum Wheat	SOM20SA3	26
Durum Wheat	SOM20SAKI1	40
Durum Wheat	SOM20SAKI3	28
Durum Wheat	SOM20SI4	12
Durum Wheat	SOM20SI3	23
Durum Wheat	SOM20SIKI3	57
Reference Material	RM 1515	51
Reference Material	RM8433	42
Reference Material	RM 1515	40
Reference Material	RM 8433	40
Blank	BLANK	0

The results show that an increasing of the Se concentration used in the soil supplementation improves the Se content in the mature grains, and that this method of supplementation is not suitable using the rates of supplementation of 4 and 20gSe/ha, since there is no increase of Se in the grain.

The yield of chemical separation of Se in the RNAA procedure was very high (mean: 98%; standard deviation: 3.4%). However, a correction for the actual yield was employed. Accuracy of the procedure was done by analyzing the reference materials NIST-SRM 1515 and NIST-SRM 8433, showing an agreement between results of this work and NIST values.

Neutron Spectrum Determination of p+Be Source Reaction for Irradiation Experiments

Laboratory of Cyclotron and Fast Neutron Generators

Milan Štefánik

Proposal ID

80

Title: **Neutron Spectrum Determination of p+Be Source Reaction for Irradiation Experiments**

Objectives: Measurement of neutron energy spectrum and fluence of p+Be source reaction up to 34 MeV

The novel high power p-Be white neutron source with neutron energy range up to 34 MeV is currently in development at the NPI Řež. This was the first experimental run of newly upgraded beryllium target station of Department of Nuclear Reactions after the technical modification of the target station head (the reduction of the shell that should led to increase the value of neutron flux). After upgrade of Be-target station, it is possible to put the irradiated samples closer to the neutron source target and thus to obtain the higher neutron flux at the position of irradiated samples. In this technical test, the neutron spectrum is determined by the dosimetry foils method in the energy range of 0.1–34 MeV.

In the irradiation experiment, the multi-foil activation technique was used to determine the neutron spectrum of the p(35)-Be source reaction at the position of irradiated samples. The set of 10 activation foils (Al, Mn, Lu, Y, Ti, Co, Bi, Fe, Au, and In) with a diameter of 15 mm and with a thicknesses in the range of 0.05 mm to 0.5 mm was irradiated at the close target-to-sample position, where the high intensity neutron flux suitable for neutron activation experiments is expected. The selected activation foils of particular materials were sensitive to various energy part of neutron spectrum according to the activation cross-sections. For the continuous neutron spectrum production at the thick Be-target, the proton beam with an energy of 35 MeV and intensity of 10 microA was used. According to Monte Carlo prediction, the neutron flux up to 10^10 neutrons/s/cm2 at the position of activation foils should be achievable – this fact should be confirmed at the end of the experimental data processing for this experimental run. After the irradiation, in dependence on half-life periods of nuclear reaction products, the activation detectors of the large dosimetry foils set were repeatedly investigated be means of nuclear gamma-spectrometry technique – gamma-spectra measurement of daughter nuclei by the semiconductor HPGe detector. Now, the gamma-spectra of the most nuclear reaction products were measured; several long-life products still remains to be measured to obtain good statistical precision. The data processing of measured activation foils has just beginning and is under process and once it will be done, the neutron spectrum reconstruction in unfolding code SAND-II with apriory information form the MCNPX simulation and measured reaction rates will be performed, and thus the neutron field at the position of irradiated samples of the newly improved Be-target will be obtained.

Graphite Powder in Al-Container

Neutron Physics Laboratory - Neutron diffraction

Stefan Seidlmayer

Proposal ID

79

Experimental Report for the Beam Time

07.11.2013 – 08.11.2013

Stefan Seidlmayer

Graphite Powder in Al-Container

Measurement of 3 samples worked as scheduled. We measured an empty container and 2 container filled with different amounts of electrode graphite powder. The container itself gave no scattering background and thus the container can be considered suitable for further experiments.

The “small” sample contained 0.1158g graphite – the “large” sample 0.1820g.

The graphite shows only a very porod like scattering (see image), even at very small angles a change in the slope is barely visible.

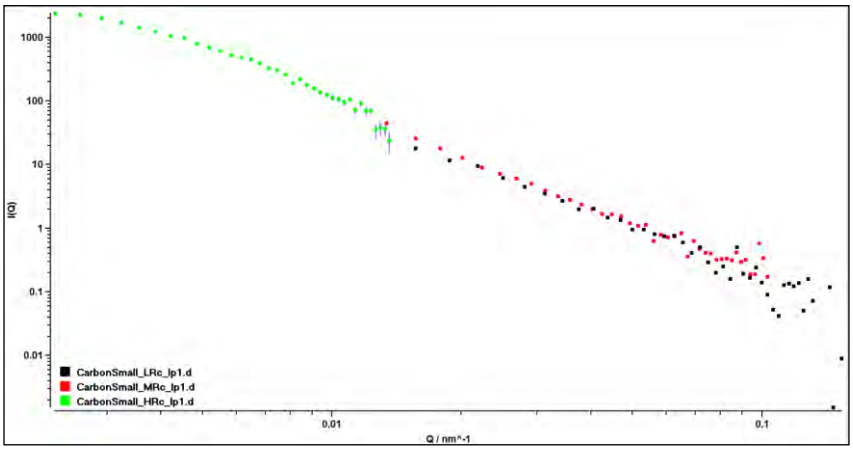

The experiment successfully proved the functionality of the intended Al-sample containers. No additional scattering contribution from the Al Container is visible.

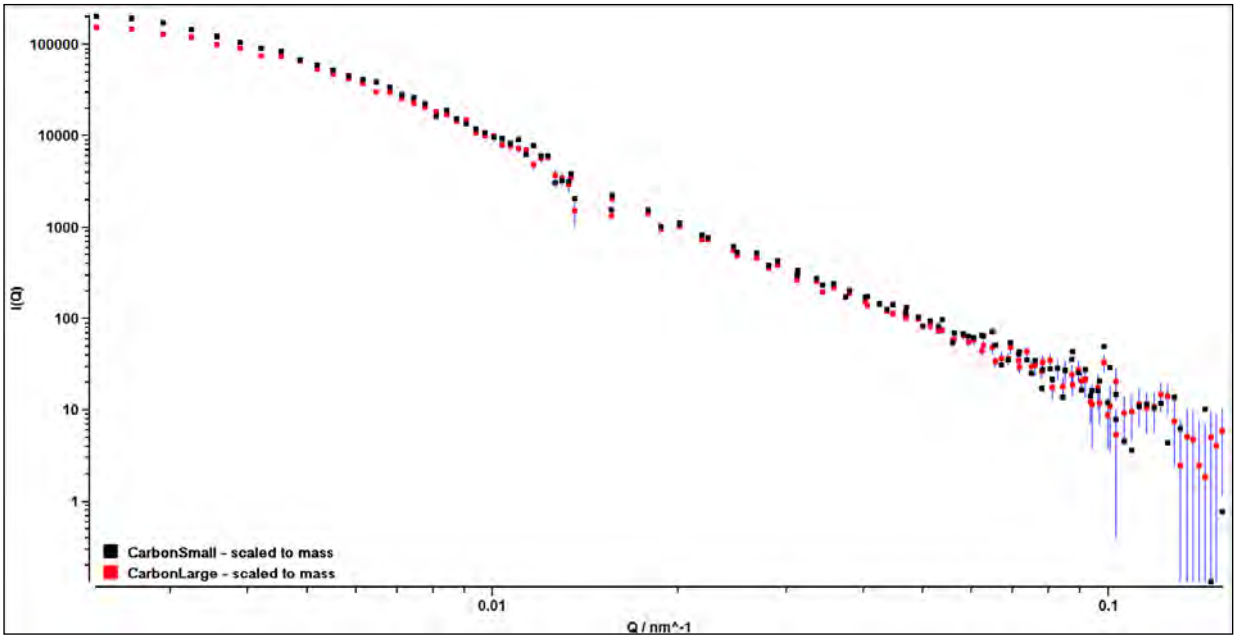

Using total sample mass for scaling has shown to work as intended for samples mounted in such a way that the entire sample is completely within the beam.

Excitation functions of p-induced reactions on nat-Nd targets in the energy range 5-12MeV + 28-38MeV

Laboratory of Cyclotron and Fast Neutron Generators

Valentina Lozza

Proposal ID

13

Report on low energy and high energy proton activation of a natural Nd target.

Valentina Lozza, Johannes Petzoldt and Kai Zuber
Technical University of Dresden, 01069 Dresden, Germany

1 Introduction

^{150}Nd is one of the preferred candidate for neutrinoless double beta decay studies, with an isotopic abundance of 5.6% and a high Q-value, above most of the natural background. Nd can be activated, while it is on the surface, by cosmic neutrons and protons. The activation products, in some cases, are long living isotopes that can be a background for the 0ν2b-decay studies. In the case of p-induced reactions most of the production cross sections were not measured before and hence a verification of the theoretical data is necessary. In order to complete the investigation reported in [1], the 28-38 MeV range, and the 5-12 MeV range are explored. The measurement were preformed at the LC of NPI-ASCR, in days from 12th to 13th of November 2012 and used as a target 4 natural Nd foils (99.9% purity, AlfaAesar) of 10x10 mm^2 and 0.1 mm thickness for the high energy range, and 4 samples of the same area but smaller thickness (about 25μm) for the low energy range. Since Nd oxidises very quickly in contact with air, the foils were covered by a thin layer of Parylene.

2 Thickness measurement

2.1 Thick natNd foils

The foil thickness was measured using low energy gamma ray (^{241}Am source) absorption at the Technical University of Dresden before the Parylene coating. To prevent oxidation the foil was measured in a mylar package under Argon atmosphere. The contribution of the mylar package was removed from the thickness measurement. Due to the large distance (more than 1 meter) between the sample and the detector (Ge-detector) the absorption coefficient with coherent scattering was used. The measurement was performed in different positions to test inhomogeneity in the foil itself. The average thickness is equal to 106±1 μm (i.e. 74.31 mg/cm^2).

2.2 Thin natNd foils

The foil thickness was measured both at the TU Dresden and at the LC institute in Řež, due to the impossibility to measure the thickness before the irradiation without opening the protective package under nitrogen atmosphere. The measurement performed at Řež, used the same Ge-detector that will be used for the activated sample counting. A special holder in lead with a pinhole (nearly 1 mm diameter) was prepared for the measurement. The thickness measured is nearly constant for the 4 thin targets, and equal to 20 μm. 5 measurements of the foils and 2 measurement of a blank were performed. The presence of the parylene coating doesn't influence the measurement of the thickness, being the absorption in parylene negligible.

3 Irradiation

Both the thin and the thick foils were measured in a stack configuration. Typical stack arrangement is given below:

- Titanium (thickness 12.11 μm) acting as a beam monitor;
- Plastic-coated neodymium foil (thickness nearly 106μm or 20μm);
- Copper beam energy degrader (Cu thickness 10.6 μm);
- Titanium (thickness 12.11 μm) acting as a beam monitor;
- Plastic-coated neodymium foil (thickness nearly 106μm or 20μm);
- Copper beam energy degrader (Cu thickness 10.6 μm);
- Titanium (thickness 12.11 μm) acting as a beam monitor;
- Plastic-coated neodymium foil (thickness nearly 106μm or 20μm);
- Copper beam energy degrader (Cu thickness 10.6 μm);
- Titanium (thickness 12.11 μm) acting as a beam monitor;
- Plastic-coated neodymium foil (thickness nearly 106μm or 20μm);
- Thick silver foil acting as a beam stop, directly cooled by water.

The first stack arrangement had the following energy at the center of each Nd foil: 35.5 MeV, 33.39 MeV, 31.37 MeV, 29.84 MeV. The irradiation lasted for 1 hour at a beam current of 0.35 μA. The beam preparation required nearly 4 hours before the measurement took place. The foils were counted overnight after the measurement. The thin foils were irradiated on the forth day for about 2 hours at a beam current of 0.35 μA. The estimated currents at the center of each foil are: 9.23 MeV, 8.09 MeV, 6.81 MeV, 5.33 MeV. The samples were counted after the irradiation in order to catch also the short living isotopes.

References:

[1] O. Lebeda et al., Phys. Rev. C 85 (2012) 014602

Assessment of the Impact of North Mara Gold Mine on River Mara Fish Contamination by Heavy Metals

Neutron Physics Laboratory - Nuclear analytical methods with neutrons

Najat Mohammed

Proposal ID

40

Samples of catfish (*Clarias mossambicus*) and lungfish (*Protopterus aethiopicus*) which are most consumed species of fish from River Mara in Tarime District of Mara Region were analyzed by INAA. Twenty samples of each fish species were collected from two sampling stations of Wegita (downstream) and Mrito (upstream) along River Mara at vicinity of North Mara Gold Mine (NMGM). The sampling stations were 70 km apart.
The samples were freeze dried, homogenized by cryogenic grinding and deep-frozen prior to analysis. Sample aliquots of approximately 100 mg and 200 mg for short-time and long-time irradiation, respectively, were sealed into acid-cleaned polyethylene disk-shaped capsules. Short- and long-time irradiations for 30 s and 3 h, respectively, were carried out in the LVR-15 reactor of the Research Centre Řež, Ltd. at neutron fluence rates of $3 \cdot 10^{13}$ cm^2 s^{-1}, $1 \cdot 10^{13}$ cm^2 s^{-1} , and $8 \cdot 10^{13}$ cm^2 s^{-1} for thermal, epithermal, and fast neutrons, respectively. Multielement standards containing known amounts of elements to be determined were simultaneously irradiated with the samples. For quality control purposes, NIST SRM 1577b Bovine Liver and NIST SRM 2711 Montana Soil were analyzed.

Counting of the irradiated samples and standards was performed in conditions given in Table 1, where t_i is irradiation time, t_d is decay time, t_c is counting time, and counting geometry is the distance of the sample from the cap of the detector. The samples and multielement standards were counted in the same geometry.

Table 1. Irradiation and counting conditions

t_i	t_d	t_c	Counting geometry	Detector[a]
30 s	10 min.	10 min.	15 cm	HPGe-1
3 h	4-5 days	1 h	20 cm	HPGe-2
	1 month	3 h	1 cm	HPGe-2

[a] HPGe-1: coaxial HPGe detector with 23 % relative efficiency, resolution FWHM 1.80 keV for the 1332.5 keV photons of ^{60}Co

HPGe-2: coaxial HPGe detector with 53 % relative efficiency, resolution FWHM 1.80 keV for the 1332.5 keV photons of ^{60}Co

The detectors were coupled to Canberra Genie 2000 computer-controlled gamma spectrometer via the chain of linear electronics, which contained a loss-free counting module (LFC Canberra 599, dual mode) to correct for the pile-up effect and dynamic changes of dead time.

Fifteen elements which are Na, Cl, K, Ca, Sc, Cr, Mn, Fe, Co, Zn, Se, Br, Rb and Sr were detected in concentration above the Minimum Detection Limit (MDL) in samples of both fish species. The concentrations of toxic elements As, Cd, Th and U were found to be below MDL of the system used in this study. In this project Hg was not detected. Most of the elements were found to be in higher concentrations in samples from downstream than upstream which might indicate contamination from the nearby Gold mine.

Composition of the newly synthesized heavy-fermion compound Ce2PtIn8

Laboratory of Tandetron

Marie Kratochvílová

Proposal ID

42

Proposal Title: Composition of the newly synthesized heavy-fermion compound Ce_2PtIn_8

The aim of this proposal was to determine the stoichiometric composition of new single Ce-*T*-In crystals we have prepared. Characterization of samples using the energy dispersive *x*-ray analysis (EDX) in the mapping mode revealed the presence of two very similar, however clearly distinguishable phases with compositions close to 2:1:8 ratios. The stoichiometry of these phases could not be determined precisely using point EDX analysis. Neither the powder nor the single-crystal *x*-ray diffraction could resolve clearly the structure of both phases. To be able to determine the compositions of both phases precisely, we applied for experiment with accelerated ions provided by LT. The sensitivity of microprobe analysis was high enough to examine the surface morphology; unfortunately, it was not able to distinguish the presence of different phases. Later, we were able to prepare single crystalline samples of Ce_2PtIn_8 and Ce_3PtIn_{11} with respect to new technological approach. The subsequent single-crystal *x*-ray diffraction and EDX analysis revealed homogeneous, single-phase composition of both tetragonal phases and thus, the issue with two phases of a very close composition within our samples (see Fig. 1) was resolved.

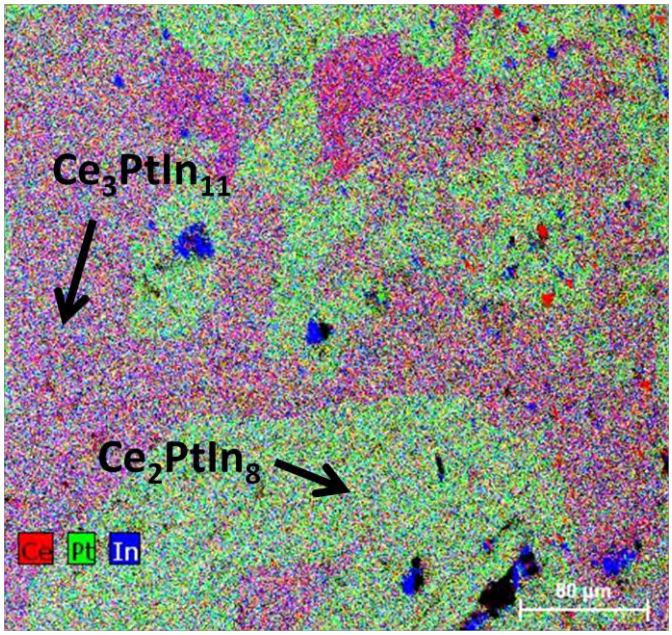

Fig. 1: EDX mapping pattern of multi-phase samples of both 2-1-8 and 3-1-11 composition. The green region represents the Ce_2PtIn_8 phase; the red region points to presence of the Ce_3PtIn_{11} phase.

Surface analysis of plasma and laser modified substrates

Laboratory of Tandetron

Petr Slepika

Proposal ID

35

The following research topics have been studied:

a) Gold nanolayer and nanocluster coatings induced by heat treatment and evaporation technique

The preparation and surface characterization of gold coatings and nanostructures deposited on glass substrate was performed. Different approaches for the layer preparation were applied. The gold was deposited on the glass with (i) room temperature, (ii) glass heated to 300°C, and (iii) the room temperature-deposited glass which was consequently annealed to 300°C. The sheet resistance and concentration of free carriers were determined by the van der Pauw method. Surface morphology was characterized using an atomic force microscopy. The optical properties of gold nanostructures were measured by UV–vis spectroscopy. The evaporation technique combined with simultaneous heating of the glass leads to change of the sheet resistance, surface roughness, and optical properties of gold nanostructures. The electrically continuous layers are formed for significantly higher thickness (18 nm), if the substrate is heated during evaporation process. The annealing process influences both the structure and optical properties of gold nanostructures. The elevated temperature of glass during evaporation amplifies the peak of plasmon resonance in the structures, the surface morphology being significantly altered. The difference in surface metal distribution of evaporated structures under RT and evaporated onto substrate heated to 300°C is evaluated in Figure 1. The difference in the behavior of surface nanostructures in area on electrical discontinuity and continuity can be clearly seen. The electrically discontinuous layer exhibits significantly higher gold concentration when deposited on non-heated substrate. The heat treatment seems to be a positive promoter of surface diffusion (and nanocluster growth), mostly in the early stages of gold layer growth. This difference, thus, seems to affect the surface gold concentration; the higher the surface concentration, the more homogeneous the layer is. On the contrary, for higher gold thicknesses, when the layer is already electrically continuous, this difference is reversed.

b) Biopolymer nanostructures induced by argon plasma irradiation and metal sputtering

Physicochemical properties of polymer surface may be modified by many techniques based on various chemical or physical processes. Modification based on polymer surface exposure to plasma irradiation exhibits an easy and cheap technique for biopolymer surface nanostructuring. By plasma exposure of polymer surface combined with consequent heating or metal deposition can be prepared materials applicable both in tissue engineering as cell carriers, but also in integrated circuit manufacturing. The influence of argon plasma irradiation on PLLA (poly(L-lactide acid) was presented. The combination of Ar+ particle irradiation, consequent sputter metallization and heating of biopolymer surface was summarized. Wettability of modified surface was characterized by the contact angle and surface energy determination. The surface morphology was studied using atomic force microscope and laser confocal microscope. The chemical analysis was performed using Rutherford Backscattering Spectroscopy (RBS) and X-ray Photoelectron Spectroscopy (XPS). The combination of plasma treatment with consequent thermal heating and/or metal sputtering led to the change of surface wettability, morphology and chemical structure. The surface roughness has been strongly influenced by the modification parameters, as well as the surface chemistry of biopolymer. The modification techniques had a positive effect on cell adhesion and proliferation.

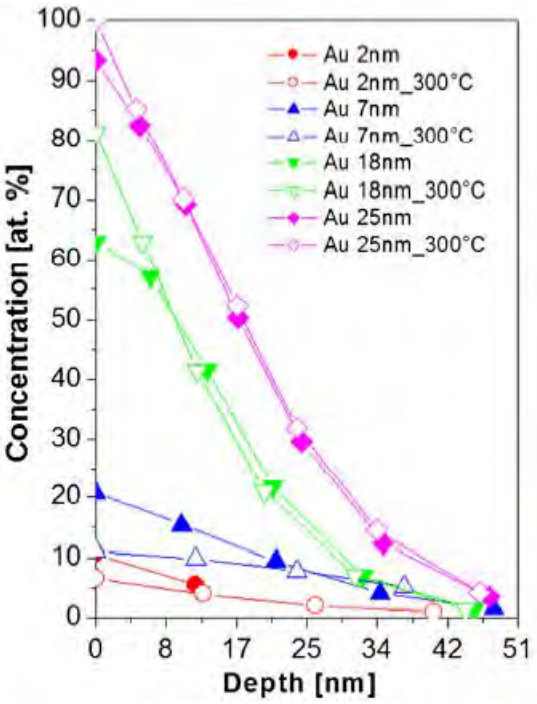

Figure 1 RBS spectra of gold structures evaporated on glass with room temperature and Au nanostructures evaporated on glass heated to 300°C (300°C).

PAPERS

1. A. Schaub, P. Slepička, I. Kašpárková, P. Malinský, A. Macková, V. Švorčík, *Gold nanolayer and nanocluster coatings induced by heat treatment and evaporation technique*, Nanoscale Res. Lett. 8 (2013) 249-257.

2. P. Slepička, P. Juřík, P. Malinský, A. Macková, N. Slepičková Kasálková, V. Švorčík, *Biopolymer nanostructures induced by argon plasma irradiation and metal sputtering*, NIM B, 2013, under review.

CONFERENCES

1. P. Slepička, P. Juřík, P. Malinský, A.Macková, N. Slepičková Kasálková, V. Švorčík, *Biopolymer nanostructures induced by argon plasma irradiation and metal sputtering*, IBA 2013 (Ion Beam Analysis), 23.6.-28.6. 2013, Seattle, USA.

2. N. Slepičková Kasálková, P. Slepička, P. Malinský, A. Macková, V. Švorčík, *Surface chamges of biopolymers induced by plasma treatment and acetone etching*, IBA 2013 (Ion Beam Analysis), 23.6.-28.6. 2013, Seattle, USA

Investigation of chemically modified carbon nanomaterials by Prompt-NAA

Neutron Physics Laboratory - Nuclear analytical methods with neutrons

Zdenek Sofer

Proposal ID

27

Project Title:**Investigation of chemically modified carbon nanomaterials by Prompt-NAA**

Proposer: Zdenek Sofer (zdenek.sofer@vscht.cz)

Lab: Neutron Physics Laboratory - Nuclear analytical methods with neutrons

The P-NAA method was used for characterization of various boron doped graphene materials. The boron doped graphene was synthesized by thermal exfoliation of various graphene oxide materials in the atmosphere of boron trifluoride diethyletherate. The incorporation of boron in graphene was investigated at various temperatures and carrier gas composition (N_2/H_2). Synthesized materials were characterized in order to evaluate chemical composition by elemental combustion analysis, X-ray photoelectron spectroscopy and X-ray florescence analysis. The boron content in the range of 20 – 560 ppm was measured by P-NAA method. The morphology of synthesized B-doped graphenes was investigated by scanning electron microscopy, transmission electron microscopy and atomic force microscopy. Transport properties were evaluated by four point probe resistivity measurement. According to rigid band model applied on these semiconductor materials we observed increase of resistivity due to the boron doping of graphene. The electrochemical performance of boron doped graphene was investigated using cyclic voltammetry in phosphate buffer (for inherent electrochemistry of B-doped graphene) and with various redox probes. The redox probes like $[Fe(CN)_6]^{3-/4-}$ was used to evaluate electron heterogeneous transfer rate on GC electrode modified with B-doped graphene. The capacitances of B-doped graphenes were evaluated from cyclic voltammetry in phosphate buffer solution. The weight specific capacitance of samples decreasing with increase of boron concentration.

The other graphene samples were prepared by chemical reduction of various graphene oxides with complex boron hydrides. The influence of graphene oxide composition on the concentration of remaining boron impurities in graphene was investigated. Significant differences were observed between graphene oxide prepared by Hofmann and Hummers methods. These results will be published in impacted journal within six months.

Published results:

1) L. Wang, Z. Sofer, P. Šimek, I. Tomandl, M. Pumera, Boron Doped Graphene: Scalable and Tunable p-Type Carrier Concentration Doping, The Journal of Physical Chemistry C, DOI: 10.1021/jp405169j.

2) H.L. Poh, P. Šimek, Z. Sofer, I. Tomandl, M. Pumera, Boron and nitrogen doping of graphene via thermal exfoliation of graphite oxide in a BF_3 or NH_3 atmosphere: contrasting properties, Journal of Materials Chemistry A, DOI: 10.1039/c3ta12460f.

Neutron diffraction on cobalt free Li-ion battery cathode materials

Neutron Physics Laboratory - Neutron diffraction

Veronika Zinth

Proposal ID

30

Neutron diffraction on cobalt free Li-ion battery cathode materials

Beamtime report
Veronika Zinth, Ralph Gilles, Premek Beran

New materials closely related to the well established NMC ($LiNi_{0.33}Mn_{0.33}Co_{0.33}O_2$) Li-ion battery material, with cobalt replaced by iron are currently studied and show promising capacities as well as cycling performance [1], [2]. To get a closer insight into structural details, $Li_{1+x}(Ni_{0.32}Mn_{0.32-y}Fe_{0.16})O_2$ samples with varying Li and Mn content were synthesized at FRM II, Germany and neutron diffraction pattern were collected at Meredith, UJF Nuclear Physics institute at a wavelength of 1.46 Å.
For $Li_{1.2}(Ni_{0.32}Mn_{0.32}Fe_{0.16})$ O2, Kartithkeyan et. al. [1] report a superstructure of the Li_2MnO_3 type in the space group C2/m that arises from ordering of additional Li and Mn in the transition metal layers, indicated by superstructure reflections in the region 20-33° 2θ (Cu-radiation). However, the neutron pattern of our samples collected at Meredith gave no indication of such superstructure reflections. Therefore, Rietveld refinement of the data was performed in the α-$NaFeO_2$-type structure (space group $R\bar{3}m$, hexagonal setting). Figure 1 and Table 1 show the results of a joint Rietveld refinement of x-ray (top, Cu- Kα_1) and neutron data (bottom).

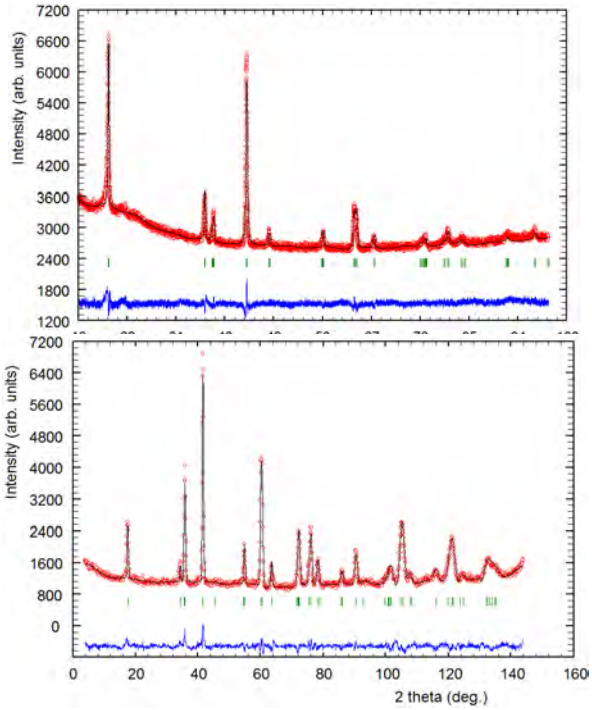

Figure 1:
Joint rietveld refinement of x-ray (Cu- Kα_1) (top) and neutron data (bottom) of $Li(Ni_{0.32}Mn_{0.28}Fe_{0.16})$ O_2

Table 1: Structural information:
Space group: $R\bar{3}m$
Lattice parameters:
a = 2.90188 Å, c = 14.34125 Å
atom sites:

Li, Ni	*3a*	0 0 0
Ni, Mn, Fe, Li	*3b*	0 0 0.5
O	6c	0 0 0.24114

Since cation mixing (of Ni and Li) is known to influence the electrochemical properties of NMC type materials [3], special attention must be paid to the occupancies of the atomic sites. While the *3a* site is mainly occupied by Li, some mixing of Ni and Li is expected because of the similar ionic radii of Ni^{2+} (0.69 Å) and Li^+ (0.76 Å) [1]. The refinement results suggest mixing of almost 13 % of Ni on the Li *3a* site. On the *3b* site, mixing of the transition metals Ni, Fe, Mn and of Li is found. With the assumption that the site is fully occupied, about 15 % Li occupy on this site. However, since no additional (superstructure) reflections can be observed in the diffraction pattern (Figure 1), the distribution of the transition metal ions and Li^+ seems to be statistical. Because four different elements occupy the *3b* site, the Rietveld refinement alone can't give sufficient information to determine the occupancies of the transition metal ions and complementary information on the elemental composition (EDX, titration) that may help to develop a suitable model is currently collected.
To summarize, high quality neutron powder data was collected at Meredith $Li_{1+x}(Ni_{0.32}Mn_{0.32-y}Fe_{0.16})O_2$ lithium ion battery materials, giving an insight into structural details and the occupancies of the atomic sites that may help to understand the electrochemical properties.

1. Karthikeyan, K., et al., Electrochimica Acta, 2012. **68**: p. 246-253.
2. Lian, F., et al., Journal of Applied Electrochemistry, 2012. **42**(6): p. 409-417.
3. Zhang, X.Y., et al., Journal of Power Sources, 2010. **195**(5): p. 1292-1301.